

Neutrinoless double-beta decay at colliders: interference between Majorana states

Jonathan L. Schubert, Oleg Ruchayskiy

Niels Bohr Institute, University of Copenhagen, Blegdamsvej 17, DK-2010, Copenhagen, Denmark

E-mail: Oleg.Ruchayskiy@nbi.ku.dk

ABSTRACT: Heavy neutral leptons (HNLs) are hypothetical particles able to explain several puzzles of fundamental physics, first and foremost — neutrino oscillations. Being *sterile* with respect to Standard Model interactions, these particles admit Majorana masses, allowing for violation of the total lepton number. Lepton number violating (LNV) processes thus become a key signature of HNLs, pursued by many experiments. In this work we demonstrate that if HNLs are the sole origin of neutrino masses, destructive interference between Majorana states suppresses the same-sign di-lepton signal. In the phenomenologically interesting case of large HNL couplings, such a suppression is akin to the cancellation of HNLs' contributions to neutrino masses. Nevertheless, the signal can be much larger than coming from the Weinberg operator alone. We identify regions of the parameter space of such realistic HNL models where the LNV signal is maximised at the LHC and future FCC-hh. Our results are obtained within the effective W approximation which allows for analytic treatment and gives a clear dependence on the model parameters. Although approximate, they are argued to be correct within a factor of few.

Contents

1	Introduction	1
2	Main idea and results	4
3	Same-sign W scattering	7
3.1	Quasi-Dirac-like model	8
3.2	Cross section of the 2-to-2 process	9
4	Results: “neutrinoless double-beta decay” at Colliders	10
4.1	Large Hadron Collider	11
4.2	Future Circular Collider	13
5	Discussion and conclusion	15
5.1	Relation between LNV effects and small neutrino masses	17
A	Type I seesaw	27
A.1	Perturbativity limit	28
B	Single HNL Case – Seesaw Line	29
C	Realistic model with two HNLs plus light Majorana states	30
D	Effective W approximation	33
E	Potential avenues for future same sign di-lepton searches at colliders	36

1 Introduction

Searches for processes forbidden by the symmetries of the Standard Model provide promising avenue of probing for new physics. Lepton Number Violating processes

(LNV) have always been among prime candidates for such searches (see e.g. [1–7]). The motivation for it comes from the century-old observation of Ettore Majorana [8] that neutral particles admit a different type of mass, *Majorana mass*. A main experimental approach to LNV searches is the neutrinoless double-beta decay ($0\nu\beta\beta$, see [9, 10] and refs. therein). Other LNV probes include experiments with muonic atoms [11] and LNV decays of mesons and τ -leptons (see e.g. [12–15]). Collider searches, such as $pp \rightarrow \ell^\pm \ell^\pm jj$ [16–26], provide a powerful tool to probe for LNV, especially in the sector involving particles other than electrons. The appeal of LNV searches lies in their potential to deduce the presence of more massive particles than can be accessed directly.

In this work we consider the *type-I seesaw model* [27–34] in which the lepton number violation comes from *heavy neutral leptons* (HNLs). The parameters of these HNLs are chosen so as to generate (Majorana) masses of neutrinos and explain neutrino oscillations. The type-I seesaw model contains two sets of Majorana particles: HNLs with masses m_{N_I} anywhere from eV to 10^{15} GeV; and mass states of active neutrinos with m_{ν_i} being in sub-eV range as dictated by neutrino oscillations [35] in combination with cosmological measurements (see [36] and references therein). HNLs interact with W^\pm , Z^0 and the Higgs boson similarly to the Standard Model neutrinos but with the couplings suppressed by the flavour-dependent mixing angles $\Theta_{\alpha I}$.¹

Many theoretical proposals on how to probe LNV signatures of HNLs have been put forward (see e.g. [37–75] for an incomplete list of references). In this work we will concentrate on a single signature of HNLs at hadron colliders: the process with two same-sign leptons and two jets (and no missing energy) in the final state, $pp \rightarrow \ell^\pm \ell^\pm jj$. The corresponding process may be mediated either via HNLs in the s -channel (Drell-Yan process, figure 1b [76, 77]) or via the direct analog of $0\nu\beta\beta$ with HNLs in t -channel — W boson fusion (WBF), figure 1a, [38–40, 46, 73]. Most of the previous LHC searches [16–26] concentrated on the process shown in figure 1b. The contribution of a single HNL to the WBF process and the corresponding Monte Carlo level analysis of the LHC sensitivity to such a signal were considered recently in [73]. It was found that the LHC sensitivity to these types of searches may be more prominent than the Drell-Yan process for HNLs with masses $m_N \gtrsim 1$ TeV. The corresponding analysis was performed recently by the CMS collaboration [78].

However, in realistic HNL models, responsible for neutrino masses, the situation is more complicated. Indeed, experimentally two mass splittings in the light neutrino mass states have been measured [35]. Therefore, *at least two* HNLs should be considered in the framework of the type-I seesaw model to explain neutrino data. This

¹Our notations: flavour index: $\alpha = \{e, \mu, \tau\}$; HNLs are enumerated with the index $I = 1, \dots, \mathcal{N}$. HNL masses: m_{N_I} ; the elements of the $3 \times \mathcal{N}$ matrix $\Theta_{\alpha I}$ describes interactions of I^{th} HNL with the flavour α .

means that even the simplest realistic model contains *four* Majorana particles: two light (active) neutrinos and two HNLs.² All these four Majorana particles contribute coherently to the same LNV process and their interference may be important.

An example of such an interplay is known from the studies of the similar process – neutrino-less double beta decay ($0\nu\beta\beta$) [9, 10]. On the one hand, the contributions to the process of light and heavy states generically interfere destructively such that the resulting signal, expressed via *effective neutrino mass* $m_{\beta\beta}$ is smaller than the one, provided by the light Majorana neutrinos alone, $m_{\beta\beta}^\nu$.³ On the other hand, enhancements of the signal as compared with $m_{\beta\beta}^\nu$ is possible for some values of HNL parameters [51, 86–88, 91–93, 97], especially if the spectrum of HNLs is hierarchical [94–96].⁴ The question, therefore, arises — *how do light and heavy Majorana degrees of freedom interplay in case of the WBF process at colliders?* Does cancellation occur between the states? Can the signal get enhanced for some values of HNL parameters? This paper is devoted to answering these questions.

Plan of the paper: The paper is organised as follows. In [section 2](#) we argue that in order to estimate the contributions of Majorana particles to the $pp \rightarrow \ell^\pm \ell^\pm jj$ cross section, it is sufficient to consider same-sign WW scattering to leptons. This makes our treatment analytic and allows to explore the dependence of the cross section on the parameters of the model. We then show that if HNLs are responsible for neutrino masses, the contributions of several HNLs can cancel each other ([appendix B](#) further substantiates this statement). Based on the analysis of [section 2](#) we can anticipate in what parts of the parameter space the cross section can nevertheless become sizeable.

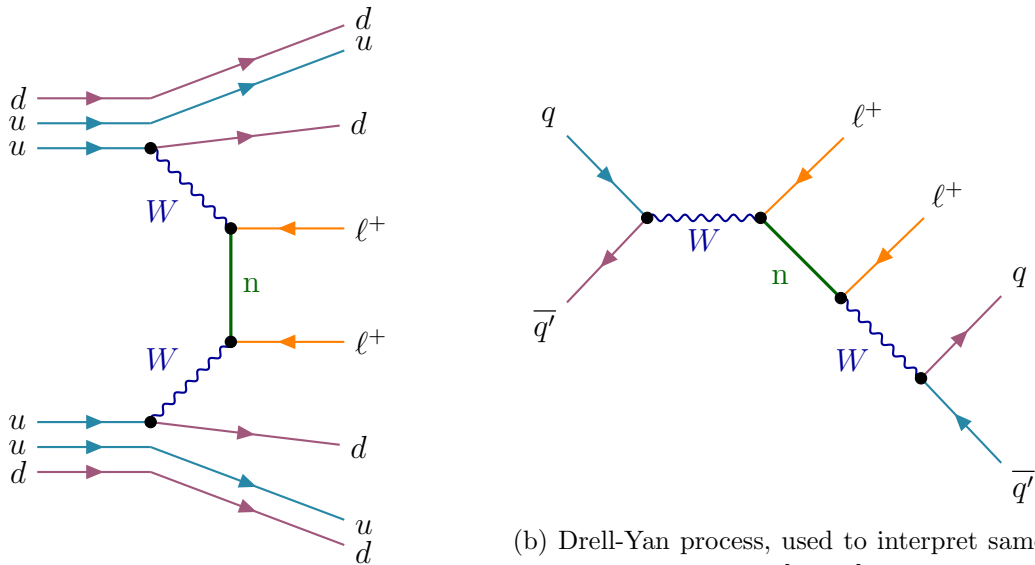
In [section 3](#) we compute same-sign WW scattering in a model with two HNLs. We show that, as expected, quasi-degenerate HNLs give negligible contribution to LNV processes, while for hierarchical HNLs the contribution can become sizeable. We substantiate the simplified treatment of [section 3](#) by exact computations in [appendix C](#).

Our results are summarised in [section 4](#). They demonstrate that the total cross section for the process $pp \rightarrow \ell^\pm \ell^\pm jj$ is at best $\mathcal{O}(1 \text{ fb})$ at $\sqrt{s_{\text{LHC}}} \simeq 13 \text{ TeV}$, making its exploration challenging even during the high-luminosity LHC (HL-LHC) phase. Owing to the higher centre of mass energy — and resultantly larger $pp \rightarrow \ell^\pm \ell^\pm jj$ cross section — we find that the proposed Future Circular Collider, during its $\sqrt{s_{\text{FCC}}} \simeq 100 \text{ TeV}$ hadron-hadron phase (FCC-hh), could produce competitive bounds in the $m_N \sim \text{few TeV}$ regime. Both these results require the HNL masses to differ

²To avoid potential confusion, we remind that in the type-I seesaw model, two non-degenerate Majorana states are sufficient to account for two light neutrino mass states. In *Inverse* [7, 79, 80] or *Linear* [81, 82] Seesaw models at least four HNLs with opposite CP phases are required.

³The literature on the subject is vast, see e.g. [83–96].

⁴This, however, may require fine-tuning between tree level and one-loop contributions to neutrino masses, see below.



(a) WBF process, reminiscent of $0\nu\beta\beta$ decay, used to interpret same-sign lepton searches in [78].

(b) Drell-Yan process, used to interpret same-sign lepton searches in [16–25].

Figure 1: Two kinds of processes leading to same-sign leptons plus jets signatures in pp collisions. Additional diagrams, originating from the interchange of the final states are not shown. The symbol n represents both light and heavy Majorana states. Panel (a): Majorana particles in t -channel (W boson fusion process). Panel (b): Majorana particles in s -channel (Drell-Yan process). The contribution from two processes are incoherent because of the antiquarks in the final state of process (b) as compared to (a).

by a factor of few.

We also discuss (section 5.1) whether, as commonly believed, LNV signals in the type-I seesaw model are proportional to neutrino masses. Appendices A, B, C and D contain additional computations as well as basic definitions, needed for completeness of our results. In appendix E we present possible points of departure for future works.

2 Main idea and results

The process in figure 1a receives contributions from all Majorana particles (HNLs and light neutrinos). An analysis of their relative contribution to the LNV processes and potential interference can be performed at the level of a $2 \rightarrow 2$ process

$$W^\pm W^\pm \rightarrow \ell_\alpha^\pm \ell_\beta^\pm \quad (2.1)$$

(where $\ell_{\alpha,\beta}^\pm$ are any of the Standard Model charged leptons, not necessarily of the same flavour). Once the cross section for the process in eq. (2.1) is known, one can

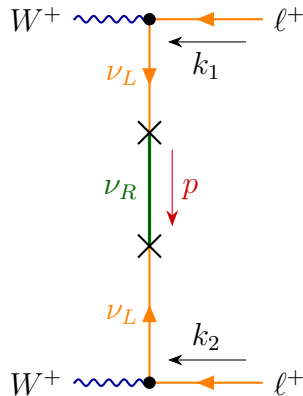


Figure 2: Feynman Diagram of the two same sign W -bosons to two same sign leptons in the flavour basis to first order in Θ^2 . The crosses mark a transition from standard model neutrino to right handed sterile neutrino, where the coupling is the Dirac mass $(m_D)_{I\ell}$.

approximately reconstruct the full $pp \rightarrow \ell_\alpha^\pm \ell_\beta^\pm jj$ cross section by using the *effective W -boson approximation* (or EWA)⁵ [98–100]:

$$\sigma(pp \rightarrow \ell^\pm \ell^\pm jj) = 2 \sum_{\substack{\lambda, \lambda' = \{T, L\} \\ \xi = \pm}} \int dx_1 dx_2 f_{W^\xi}^\lambda(x_1) f_{W^\xi}^{\lambda'}(x_2) \sigma^{\lambda\lambda'}(W^\xi W^\xi \rightarrow \ell^\xi \ell^\xi)(x_1 x_2 s_{pp}). \quad (2.2)$$

where x_1, x_2 are the W 's Björken x , s_{pp} is the pp centre of mass energy, and the sum goes over both signs of W -bosons (ξ) as well as the transversal (T) and longitudinal (L) polarizations.

In this approximation, W -bosons are treated as polarised partons, and the pp level cross section is derived by folding the polarised cross sections of the WW scattering process, $\sigma^{\lambda\lambda'}(W^\pm W^\pm \rightarrow \ell^\pm \ell^\pm)$, with the corresponding parton distribution functions (PDFs) $f_{W^\pm}^\lambda(x)$. More details are provided in the Appendix D. The caveats and limitations of this approximation have been recently analysed in [101] (see also [100, 102]).

Going fast-forward, the results of our analysis are shown in section 2 in terms of parameter exclusion on the HNL mixing angle $\Theta_{\ell 1}$ at 95% C.L. without detector cuts and assuming background-free searches for the high-luminosity LHC phase and FCC-hh. The details and assumptions that went into these exclusion limits are presented in sections 3 and 4 below. For a qualitative discussion of these results see section 5.

⁵The PDFs of this approximation are derived at leading QCD order, but includes further approximations (for discussion see appendix D). Monte Carlo studies [73] demonstrate that the k -factor (NLO vs. LO correction) is $\lesssim 1.5$ for the processes in question, supporting this approach.

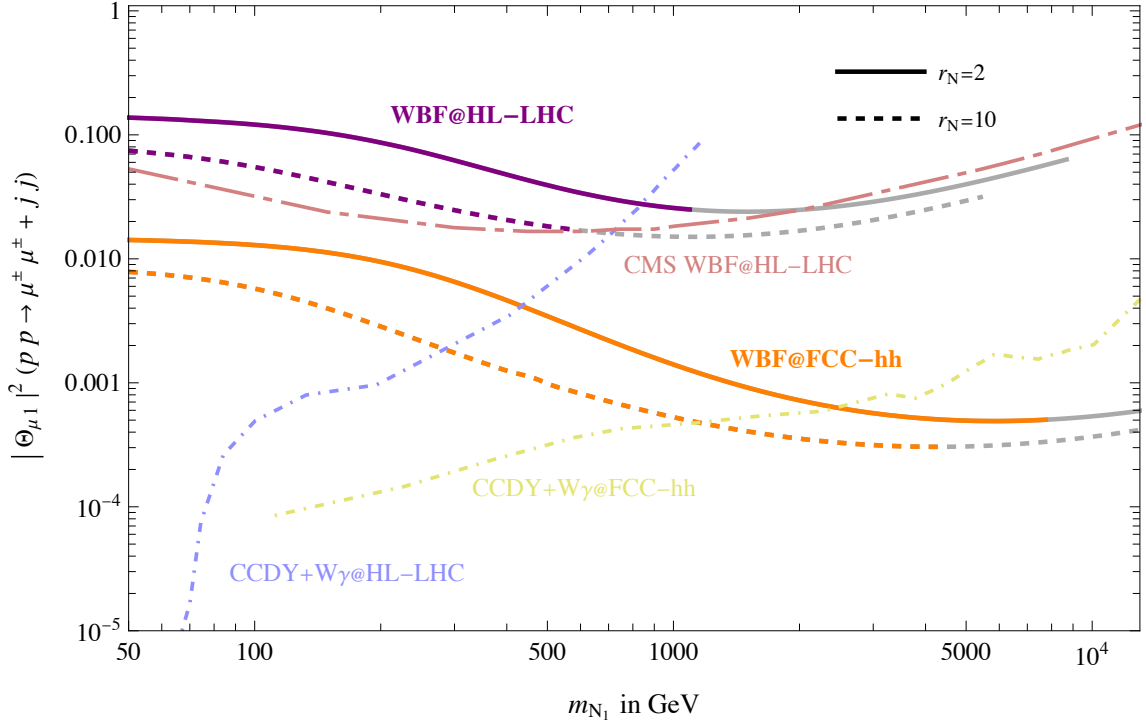


Figure 3: Exclusion limits on the HNL mixing angle for WBF-mediated process $pp \rightarrow \mu^\pm \mu^\pm + jj$ at the HL-LHC and FCC-hh (purple and orange lines). The results are presented for two HNLs whose mass ratio equals to r_N , with $\Theta_{\ell 1}$ being the mixing angle of the lighter HNL (see in-plot legends). The long-short dashed line indicates the rescaling of the recent CMS dilepton search [78] to HL-LHC phase (red-grey). Short dash-dotted “CCDY + $W\gamma$ ” lines are extrapolations of the CMS tri-lepton searches [103] based on [104] (light blue) and a MG5_AMC simulation based on the ATLAS detector [105] (yellow-grey). All limits are at 95% C.L. Grey ends of the orange and purple curves correspond to Yukawa couplings approaching non-perturbative values $1 < |F_{\ell 1}| < 4\pi$. See text for details.

The qualitative analysis of the matrix element for eq. (2.1) is most readily performed in the *flavour basis*. In this case only the right-chiral neutrinos ν_R contain a Majorana mass term.⁶ Therefore, analysis of the diagram in figure 2 includes all contributions and interference terms.

The amplitude of the $W^\pm W^\pm \rightarrow \ell^\pm \ell^\pm$ subprocess shown in figure 2 is written as

$$\mathcal{M}_{\text{ww}}^{\mu\nu} = -i \frac{g^2}{2} \bar{u}(k_2) \gamma^\mu P_R \frac{1}{\not{p}} \sum_I \left[(m_D)_{\alpha I} \frac{\not{p} + m_{N_I}}{p^2 - m_{N_I}^2} (m_D)_{\beta I} \right] \frac{1}{\not{p}} \gamma^\nu P_L v(k_1) + (k_1 \leftrightarrow k_2). \quad (2.3)$$

here g is the weak coupling constant, $P_{R,L}$ are chiral projectors, u, v are spinors

⁶Section 3 below substantiates these arguments by proper computation in the mass basis.

of the outgoing leptons. Dirac (m_D) and Majorana (m_{N_I}) masses are defined in [appendix A](#). We have implicitly chosen a counterclockwise evaluation direction, the effects of which — according to the Feynman rules for fermion number violating interactions [106] — are twofold:

- The spinor associated with the fermion going against the chosen direction is charge conjugated.
- The chiral projector in the vertex connecting to this fermion is transformed according to $\Gamma' = C\Gamma^T C^{-1}$, where C is the charge-conjugation matrix.

These rules result in the cancellation of the \not{p} term in the numerator of [eq. \(2.3\)](#), so that the amplitude is proportional to m_{N_I} . This cancellation can be anticipated from the fact that LNV effects are enabled solely by the existence of the Majorana mass. We can rewrite [eq. \(2.3\)](#) in the compact form

$$\mathcal{M}_{\text{ww}}^{\mu\nu} = -i\frac{g^2}{2} \left(\bar{u}(k_1)\gamma^\mu\gamma^\nu P_L v(k_2) \right) \times \sum_I \Theta_{\alpha I} \Theta_{\beta I} \left[\frac{m_{N_I}^3}{t(t - m_{N_I}^2)} - (t \leftrightarrow u) \right], \quad (2.4)$$

where t and u are Mandelstam variables.

At this stage we can already anticipate an answer to the questions raised in [section 1](#): In the limit $|t|, |u| \ll m_{N_I}^2$, the sum in [eq. \(2.4\)](#) reduces to the seesaw expression (see [appendix A](#)):

$$m_{\alpha\beta}^{(\nu)} \equiv \sum_{i=1}^3 V_{\alpha i} m_i V_{\beta i} = - \sum_I \Theta_{\alpha I} \Theta_{\beta I} m_{N_I}. \quad (2.5)$$

where $V_{\alpha i}$ are PMNS matrix elements and m_i are light neutrino masses. This means that for very heavy HNLs the total cross section will be proportional to the neutrino masses, i.e. will be unobservable.

Similarly, for *almost degenerate* HNLs ($m_{N_1} \simeq m_{N_2} = m_N$) [eq. \(2.4\)](#) becomes proportional to a linear combination of $m_N \sum_I \Theta_{\alpha I} \Theta_{\beta I}$ which again reduces to the light neutrino mass matrix (2.5). This result is not surprising, as for two quasi-degenerate HNLs the total lepton number becomes conserved [107, 108].

However, in the case where $|t|, |u| \sim m_{N_I}^2$ and/or HNLs are non-degenerate, [eq. \(2.4\)](#) does not readily reduce to the seesaw relation and thus is not proportional to the neutrino masses. Hence, *one can expect that the largest LNV effect can be achieved for the HNLs with hierarchical masses*. The following sections substantiate this claim.

3 $W^\pm W^\pm \rightarrow \ell^\pm \ell^\pm$ scattering in the model with two HNLs

HNLs with mass m_{N_I} and coupling $\Theta_{\ell I}$ contribute to neutrino mass matrix at the level $\Theta_{\ell I}^2 m_{N_I}$. Therefore, to be consistent with neutrino data, one has two distinct

possibilities: either mixings $\Theta_{\ell I}$ are close to the *seesaw line* (see [Appendix A](#)):

$$|\Theta_{\ell I}|^2 \sim 5 \times 10^{-14} \left(\frac{\text{TeV}}{m_{\text{N}}} \right), \quad (3.1)$$

or several HNLs cancel each other's contributions to neutrino masses [[107](#), [108](#)]. This latter case is phenomenologically interesting, as HNL mixings can exceed the naive limit [\(3.1\)](#) by orders of magnitude, making them accessible for direct searches. We will, therefore, concentrate on this case.

3.1 Quasi-Dirac-like model – two HNLs with cancelling contribution to neutrino mass

To simplify our treatment, we arrange the HNL mixing angles in such a way that the individual contributions to the light neutrino masses cancel:^{[7](#)}

$$0 = m_{\ell\ell}^\nu = \sum_{I=1}^2 \Theta_{\ell I}^2 m_{\text{N}_I}. \quad (3.2)$$

This allows getting rid of light neutrino contributions and analysing only interference between HNL states. We will see below that the contribution to the WBF process will be non-zero in this case, because for large HNL mixings, neutrino contributions are subdominant. The effect from light neutrino masses is presented in [appendix C](#). Finally, this parameter choice also allows us to demonstrate that LNV can be prominent, even if neutrino masses are zero.

In the context of 2 HNLs, [eq. \(3.2\)](#) can be satisfied by the prescription of

$$\Theta_{\ell 2} = \pm i \Theta_{\ell 1} \sqrt{\frac{m_{\text{N}_1}}{m_{\text{N}_2}}} = \pm i \frac{\Theta_{\ell 1}}{\sqrt{r_{\text{N}}}}, \quad (3.3)$$

where we have introduced the *mass ratio*

$$r_{\text{N}} \equiv \frac{m_{\text{N}_2}}{m_{\text{N}_1}} \geq 1. \quad (3.4)$$

We will refer to the HNL pair obeying [eq. \(3.3\)](#) with $r_{\text{N}} > 1$ as the *quasi-Dirac-like* (QDL) model.

In the limit of $r_{\text{N}} \rightarrow 1$, known as the *Dirac-limit*, the two HNLs will form a single Dirac fermion. As a consequence, SM lepton number is conserved and the LNV effects will cancel entirely. This is not the case if $r_{\text{N}} > 1$ where, as we will see, LNV effects are non-zero. The QDL model produces realistic predictions in the large mixing angle regime, which we will present in the following. By comparison, the effect of light neutrino masses is marginal (presented in [Appendix C](#)).

⁷In this Section we ignore the flavour structure and consider a generic flavour ℓ .

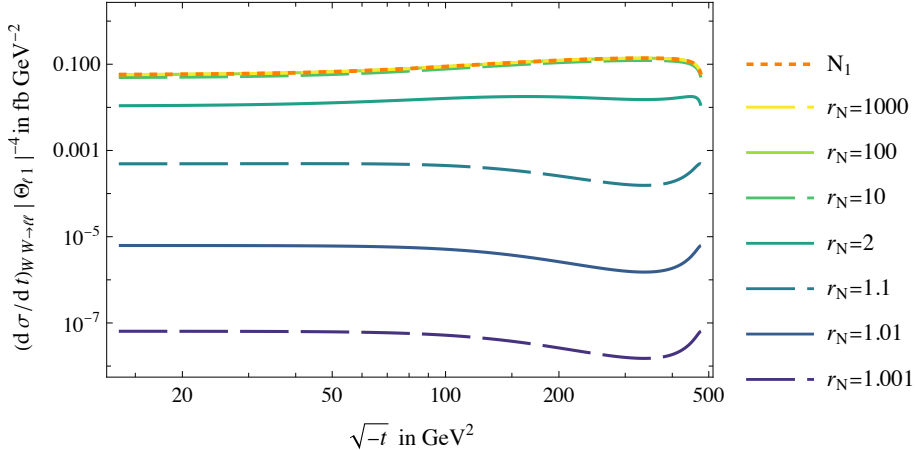


Figure 4: Differential cross section of $W^\pm W^\pm \rightarrow \ell^\pm \ell^\pm$ scattering in a model with two HNLs with cancelling contributions to the light neutrino masses (QDL). The lighter HNL mass is kept at $m_{N_1} = 150$ GeV, while the heavier one is determined by the mass ratio r_N , see eq. (3.4). The mixing angle suppression $|\Theta_{\ell 1}|^4$ is factored out of the result. The mass of the final leptons ℓ is neglected. The centre of mass energy is 500 GeV.

3.2 Cross section of the $W^\pm W^\pm \rightarrow \ell^\pm \ell^\pm$ process

The $W^\pm W^\pm \rightarrow \ell^\pm \ell^\pm$ cross-section depends on the WW centre of mass energy $\sqrt{s_{\text{WW}}}$. This variable corresponds to $x_1 x_2 s$ in the EWA approximation formula (2.2). In the following we set $\sqrt{s_{\text{WW}}} \simeq 500$ GeV which represents a typical value for the invariant mass of the WW system in pp scattering at the 13 TeV LHC (c.f. [73]).

Averaging over W polarisations contracted with the amplitude in eq. (2.3) we can find the differential cross section of the $W^\pm W^\pm \rightarrow \ell^\pm \ell^\pm$ process which is shown for different mass ratios (viridis colour scheme) in figure 4. As expected, the differential cross section decreases as $r_N \rightarrow 1$ approximately as $d\sigma/dt \propto (r_N - 1)^2$. The process fully vanishes in the case of exact HNL pair degeneracy (quasi-Dirac limit). For $r_N \gg 1$, the differential cross section in the two HNL model approaches that of a single isolated HNL N_1 (dashed orange), so that from $r_N = 10$ the two become indistinguishable at the scales shown here. This is due to the fact that for large HNL masses ($m_{N_2}^2 \gtrsim |t|_{\text{max}}$) the denominator of the heavier HNL propagator is always dominated by the mass term, suppressing all N_2 contributions by at least r_N^{-1} . For all r_N , the numerical value of the cross section is of the same order of magnitude for all t . This corresponds to an evenly distributed angular dependence of the ejectiles. However, we do observe that for a QDL pair closer to degeneracy, there is a slight tendency toward back-to-back scattering. The opposite is true for a highly hierarchical configuration.

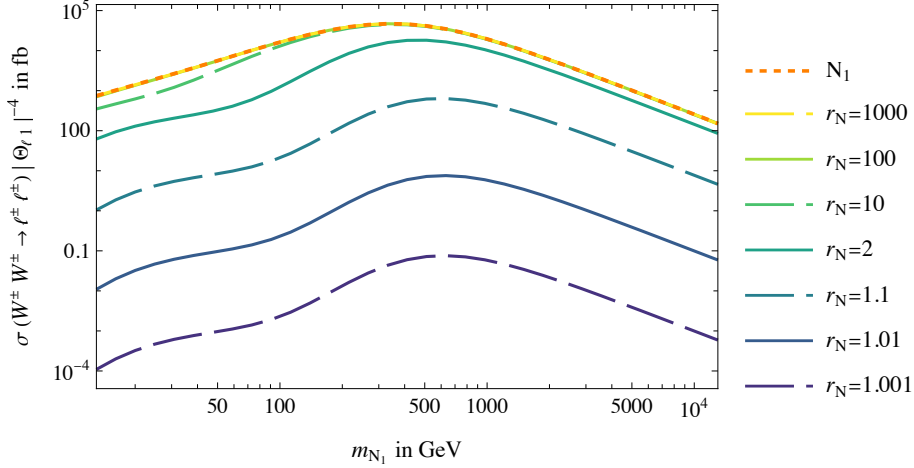


Figure 5: Total cross section of $W^\pm W^\pm \rightarrow \ell^\pm \ell^\pm$ scattering in a model with two HNLs with cancelling contributions to the light neutrino masses (qDL). The cross section is divided by $|\Theta_{\ell 1}|^4$. The mass of the lighter HNL is shown as the x-axis, while the heavier one is r_N times larger. The masses of the final leptons ℓ are neglected.

Figure 5 shows the total cross section of $W^\pm W^\pm \rightarrow \ell^\pm \ell^\pm$ as a function of the lighter HNL mass m_{N_1} . For masses $m_{N_1} \lesssim \sqrt{s_{\text{WW}}}/10 \simeq 50$ GeV we see a difference between hierarchical HNLs with $r_N \sim 10$ and the single HNL case. This is due to m_{N_2} being smaller than $\sqrt{s_{\text{WW}}}$ in this regime, so that $m_{N_2}^2 \lesssim |t|_{\text{max}}$ and decoupling of a heavier HNL does not happen. Hence, a cancellation between the two contributions can occur.

The overall shape of the total cross section, as a function of mass m_{N_1} , exhibits maximal value for $m_{N_1} \sim \sqrt{s_{\text{WW}}}$. Trends for small and large m_{N_1} can be directly understood from the amplitude in eq. (2.3) of the $W^\pm W^\pm \rightarrow \ell^\pm \ell^\pm$ process, which at small mass scales as m_{N_1} . At large masses it is suppressed as $m_{N_1}^{-1}$, which can also be observed in the cross section.

We note that the cross section in a realistic qDL model can be substantially larger than that in a single HNL model with the mixing angles close to the seesaw line (see Appendix B).

4 Results: “neutrinoless double-beta decay” at Colliders

Using the effective W approximation, the results of the previous section are translated into pp level cross sections. Although our results were obtained in the qDL model (i.e. in the limit where HNLs’ contribution to neutrino masses cancels exactly even if $m_{N_1} \neq m_{N_2}$), they are valid in realistic 2HNL models with non-zero neutrino masses. In appendix C, it is demonstrated that far from the seesaw line ($|\Theta_{\ell I}| \gg |\Theta|_{\text{seesaw}}$,

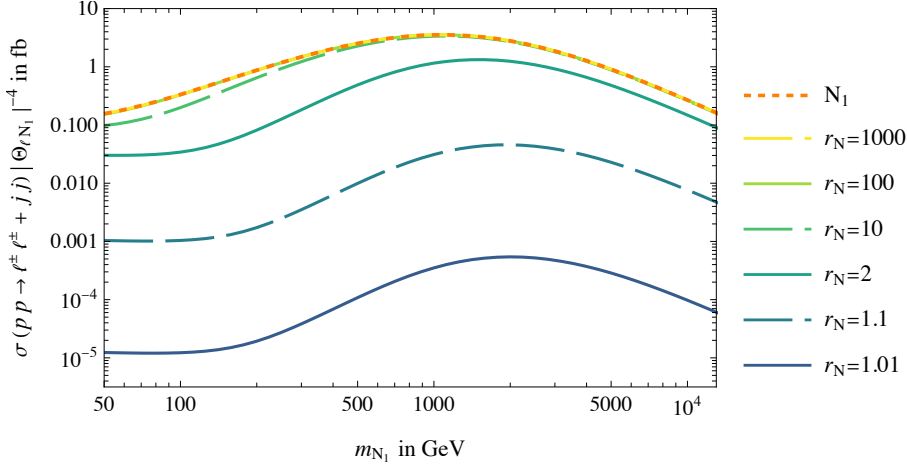


Figure 6: Cross section of $pp \rightarrow \ell^\pm \ell^\pm jj$ as calculated in the effective W approximation in the model with two HNLs whose mass ratio is equal to r_N . The mass of the lighter HNL is shown as the x-axis, while another one is r_N times heavier. Notations are the same as in [figure 5](#). The dependence on the mixing angle $|\Theta_{\ell 1}|^4$ is factored out. Contribution of the light neutrinos is neglected (see [section 3](#) for details). The centre of mass energy is assumed to be $\sqrt{s_{\text{LHC}}} = 13 \text{ TeV}$.

the light neutrino’s contributions to the process become negligible compared to those of the HNLs. As we will see, only HNLs with large mixing angles could lead to detection of WBF at the LHC or FCC-hh, so that it is justified to consider the QDL model.[§] This makes numerical integration of the relevant matrix elements simpler and numerically stable.

4.1 Large Hadron Collider

[Figure 6](#) shows the expected total cross section of $pp \rightarrow \ell^+ \ell^+ + jj$ for a centre of mass energy $\sqrt{s_{\text{LHC}}} = 13 \text{ TeV}$. We remind that the effective W approximation largely underestimates the cross-section for masses *below few hundred GeV* (see [appendix D](#) below) and therefore our results only apply for larger masses. Compared to [figure 5](#) we see that the polarisation decomposition and subsequent folding with the W PDFs shifts the maximum from around $m_{N_1} \sim 0.5 \text{ TeV}$ to $m_{N_1} \sim 1 \text{ TeV}$. More importantly, the pp cross section is about 4 orders of magnitude smaller than that of the WW . Beyond this, the general characteristics of the WW -scattering case are directly translated into the pp case. Using the pp cross sections from [figure 6](#), we can estimate how many LNV events could be expected at the LHC. To this end, we multiply the

[§]We also repeated our analysis for a single HNL in a model ignorant of light neutrino masses. At WW level, our results match those of [\[73\]](#) while at pp level they differ by a factor of ~ 1.6 in the region of full validity according to [appendix D](#). The origin of this factor could be related to known limitations of EWAs, see [\[101\]](#) for detailed discussion.

cross section by the maximal *admissible value* of the mixing angles (see [appendix A](#) for details). Namely, *each mixing angle* $\Theta_{\ell 1}$ and $\Theta_{\ell 2}$ should obey the condition

$$|\Theta_{\ell I}| \leq \begin{cases} 1, & m_{N_I} < \text{vev} \\ \frac{\text{vev}}{m_{N_I}}, & m_{N_I} > \text{vev} \end{cases} \quad (4.1)$$

for its respective mass. Notice that for $m_{N_2} > \text{vev}$ and $r_N > 1$, the perturbativity condition of the HNL N_2 provides the most stringent theoretical upper bound on $|\Theta_{\ell 1}|$ (under the assumption of [eqs. \(3.2\)](#) to [\(3.3\)](#)).⁹

[Figure 7](#) shows the expected maximal amount of events N_{max} at the HL-LHC with an integrated luminosity of $3000 \text{ fb}^{-1} \equiv 3 \text{ ab}^{-1}$ [[111](#)] as a function of the lighter of two HNL masses m_{N_1} for different mass ratios r_N , as well as for a single HNL case (dashed orange). The number of events reaches its maximum at $m_{N_1} \sim \text{vev}/r_N^{1/2}$. For models with $m_{N_1} < 100 \text{ GeV}$, N_{max} is the largest for $r_N \gtrsim \mathcal{O}(10)$, while for $m_{N_1} > 100 \text{ GeV}$ N_{max} is largest for $r_N \sim \text{few}$. Notice that the differential cross section for $r_N \geq 2$ looks similar to that of the single HNL. Therefore, efficiencies of cuts will be similar to those estimated in [[73](#)].¹⁰ We stress that for all mass ratios $N_{\text{max}} < 1$ for $m_{N_1} \geq 1.2 \text{ TeV}$ and that the region above 1 TeV can only be probed for $2 \leq r_N \lesssim 10$.

Furthermore, we can estimate 95% CL exclusion in the $(\Theta_{\ell N}, r_N, m_N)$ parameter space. Below we report our results for $r_N = 2$ and $r_N = 10$, as they represent the most promising mass ratio regime according to [figure 7](#). Bounds for $r_N < 2$ quickly deteriorate $|\Theta_{\ell N}|_{95\%}^2 \propto |r_N - 1|^{-1}$. For $r_N > 10$ growing fraction of the parameter space becomes excluded due to perturbativity constraints, [Section A.1](#). In a model with $r_N \sim \text{few}$ ([figure 8a](#)), and 100% efficiency ($\epsilon \sim 1$, yellow), we find that a WBF search at the HL-LHC can probe HNL masses m_{N_1} up to 1 TeV. This mass range is limited to $m_{N_1} \lesssim 500 \text{ GeV}$ for a lower efficiency ($\epsilon \sim 0.1$, dashed grey). In a model with $r_N \sim \mathcal{O}(10)$ ([figure 8b](#)) the cross section per $|\Theta_{\ell 1}|^4$ is higher, but the range of accessible masses is smaller, due to the perturbativity condition of [eq. \(4.1\)](#). As a result the maximally probed HNL mass is $m_{N_1} \lesssim 500 \text{ GeV}$. This limit drops to around 300 GeV for a lower efficiency. With efficiency dropping to $\epsilon \sim \mathcal{O}(10^{-2})$, a signal cannot be expected for any meaningful $(\Theta_{\ell N}, r_N, m_N)$ combination.

⁹This, in particular, demonstrates that decoupling of one of the HNLs, while keeping neutrino masses small is not possible – the condition for the theory to remain perturbative imposes constraints on the mixings of non-decoupled lighter HNLs. This is an example of the known violation of the “decoupling theorem” [[109](#)] in type-I seesaw model, see e.g. recent discussion in [[110](#)].

¹⁰For masses $m_{N_1} \sim \text{few TeV}$ this corresponds to a signal loss of around 40%.

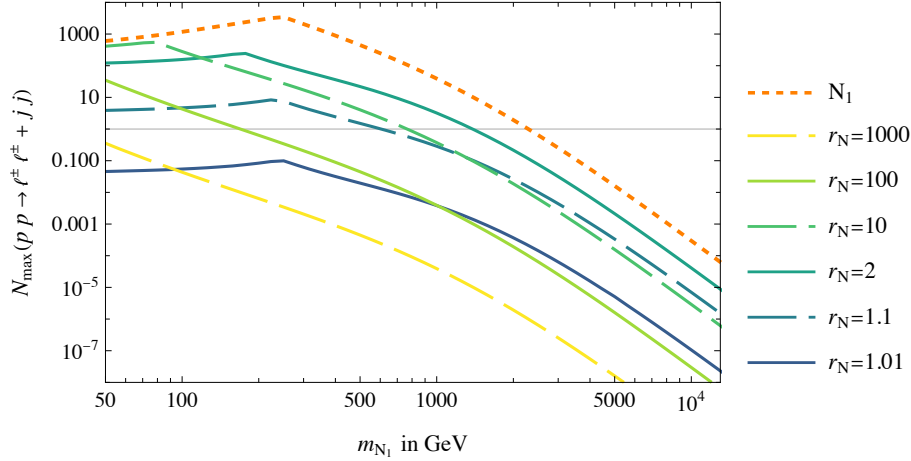


Figure 7: The maximal number of WBF events as calculated in the effective W approximation in the model with two HNLs with mass ratio r_N . The mixing angle $|\Theta_{\ell l}|^4$ is maximised, according to eq. (4.1). Notice that for $m_{N_2} = r_N m_{N_1} > \text{vev}$, it is the condition on the mixing angle $|\Theta_{\ell 2}|$ that dominates. The overall efficiency of the signal is assumed 100%. The centre of mass energy is $\sqrt{s_{\text{LHC}}} = 13 \text{ TeV}$ and the luminosity 3 ab^{-1} .

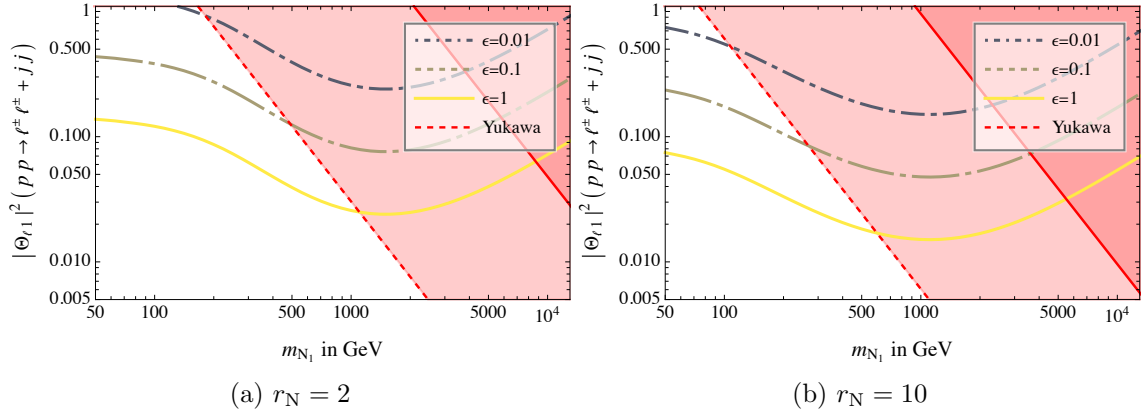


Figure 8: *Optimistic* exclusion limits on the N_1 parameters via WBF-mediated $pp \rightarrow \ell^\pm \ell^\pm jj$ events in the model with two HNLs with mass ratio r_N . The dashed red line indicates the perturbativity limit of the Yukawa coupling $|F_{\ell 2}| = 1$, while the solid red line indicates $|F_{\ell 2}| = 4\pi$. The exclusion limits are 95% CL assuming zero background. The centre of mass energy is $\sqrt{s_{\text{LHC}}} = 13 \text{ TeV}$ and the luminosity 3 ab^{-1} .

4.2 Future Circular Collider

Sensitivity of the WBF process is maximal for $\sqrt{s_{\text{WW}}} \sim m_{N_1}$. The former increases with the \sqrt{s} of pp collision. Therefore the process under consideration can be ex-

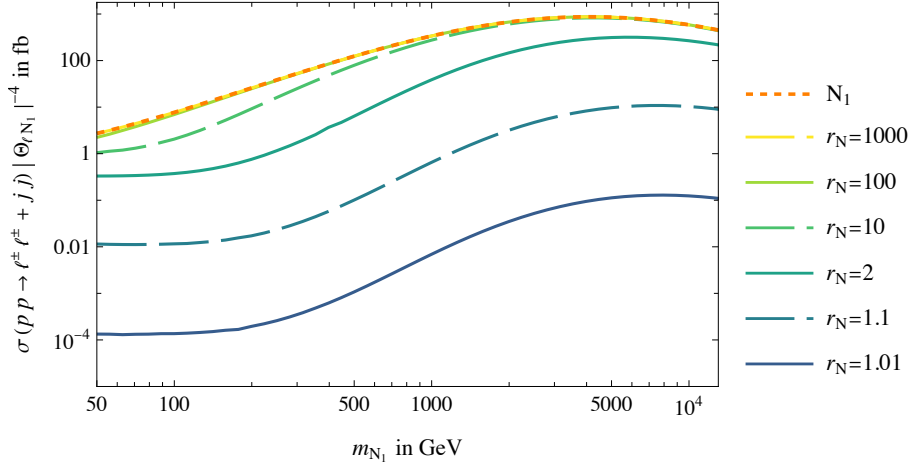


Figure 9: Cross section of $pp \rightarrow \ell^\pm \ell^\pm jj$ as calculated in the effective W approximation in the model with two HNLs whose mass ratio is equal to r_N . The mass of the lighter HNL is shown as the x-axis, while another one is r_N times heavier. Notations are the same as in [figure 5](#). The dependence on the mixing angle $|\Theta_{\ell 1}|^4$ is factored out. Contribution of the light neutrinos is neglected (see [section 3](#) for details). The centre of mass energy is assumed to be $\sqrt{s_{\text{FCC}}} = 100$ TeV.

pected to be more efficient at the Future Circular Collider in the pp mode (FCC-hh) [[112](#)]. Using its projected centre of mass energy $\sqrt{s_{\text{FCC}}} = 100$ TeV and machinery, developed in this work, we can estimate the cross section of the $pp \rightarrow \ell^\pm \ell^\pm jj$ process, shown in [figure 9](#).

We find that the cross section reaches its maximum at $m_{N_1} \simeq 2\text{--}3$ TeV (compared to $m_{N_1} \simeq 1\text{--}1.5$ TeV at LHC energies). It is, furthermore, ~ 2.5 orders of magnitude larger at FCC energies and reaches ~ 1 pb for a hierarchical HNL pair.

With a target integrated luminosity 30 ab^{-1} [[113](#)], this corresponds to a maximal theoretically admissible event number N_{max} as shown in [figure 10](#). Again, we see that for $m_{N_1} > r_N^{-1/2} \text{ eV}$ Yukawa perturbativity becomes the main theoretical constraint on the mixing angle $\Theta_{\ell 1}$, resulting in $r_N \sim \text{few}$ to yield the largest N_{max} .

Due to the significantly larger cross section and higher integrated luminosity, the relevant $(\Theta_{\ell N}, r_N, m_N)$ parameter space covered by $pp \rightarrow \ell^\pm \ell^\pm jj$ at the FCC-hh opens up. For both $r_N = 2$ and $r_N = 10$ (see [figures 11a](#) and [11b](#) respectively), physically relevant mixing angles $\Theta_{\ell N}$ are within reach for a qDL HNL pair with $m_{N_1} \sim \text{few}$ TeV assuming a detection efficiency $\epsilon \geq 0.1$.

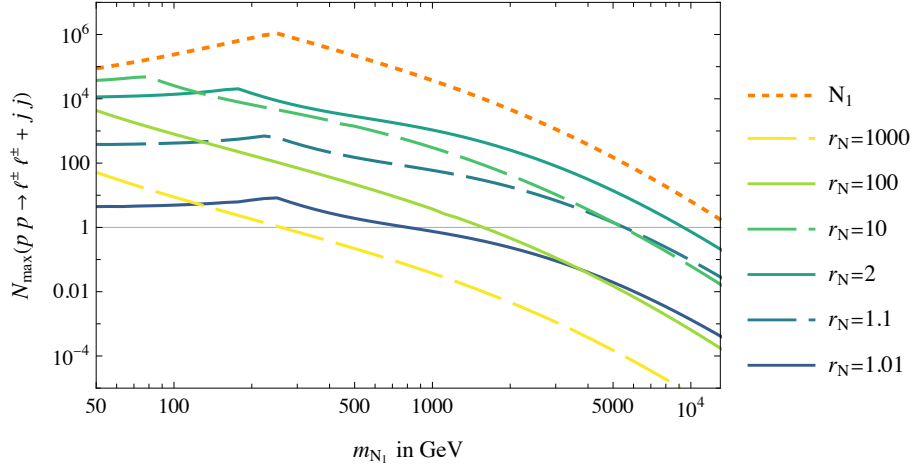


Figure 10: The maximal number of WBF events as calculated in the effective W approximation in the model with two HNLs with mass ratio r_N . The mixing angle $|\Theta_{\ell 1}|^4$ is maximised, according to eq. (4.1). Efficiency of the detector is assumed 100%. The centre of mass energy is $\sqrt{s_{\text{FCC}}} = 100$ TeV and the luminosity 30 ab^{-1} .

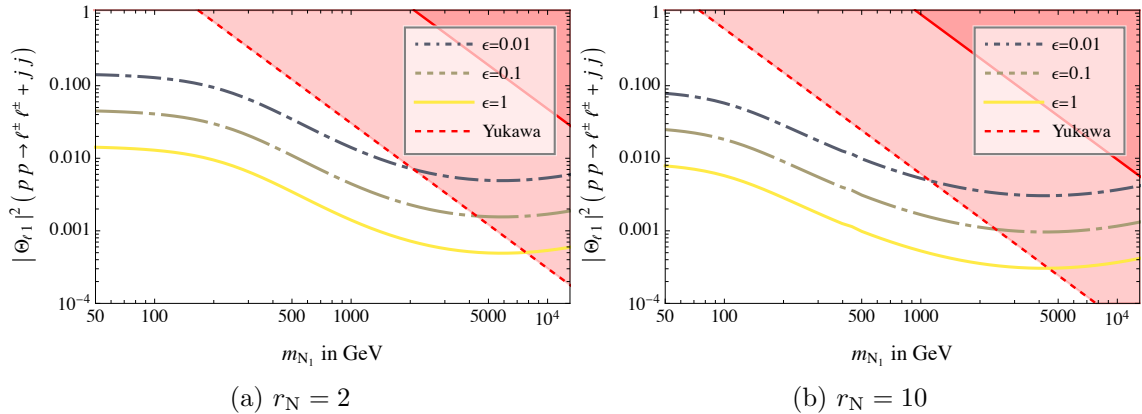


Figure 11: *Optimistic* exclusion limits on the N_1 parameters via WBF-mediated $pp \rightarrow \ell^\pm \ell^\pm jj$ events in the model with two HNLs with mass ratio r_N . The dashed red line indicates the perturbativity limit of the Yukawa coupling $|F_{\ell 2}| = 1$, while the solid red line indicates $|F_{\ell 2}| = 4\pi$. The limits are obtained for 95% CL exclusions assuming zero background. The assumed detector efficiency is ϵ , the centre of mass energy $\sqrt{s_{\text{FCC}}} = 100$ TeV and the luminosity 30 ab^{-1} .

5 Discussion and conclusion

In this work we analysed the collider probe for Majorana particles with masses ranging from ~ 50 GeV to ~ 5 TeV. The process that we considered is a direct analog of the $0\nu\beta\beta$ decay — $pp \rightarrow \ell^\pm \ell^\pm jj$ (figure 1a). Compared to previous works on the subject (c.f. [37, 40, 59, 73, 114]) we concentrated on models where HNLs are solely re-

sponsible for generating neutrino masses. All Majorana particles — HNLs and active neutrinos — contribute to the process in question and we analysed their interference. We demonstrated that such an interference is necessarily *destructive* as a consequence of smallness of neutrino masses, as compared to other relevant energy scales. There are two limiting regimes depending on whether HNLs’ mixing angles $|\Theta_{\ell N}|$ are comparable or much larger than the naive “seesaw limit” $|\Theta|_{\text{seesaw}}^2 = \frac{\sqrt{|\Delta m_{\text{atm}}^2|}}{m_N}$ (see text around eq. (A.8))

1. For $|\Theta_{\ell N}| \sim |\Theta|_{\text{seesaw}}$ cancellation between HNLs and neutrino states can occur and the resulting cross section is proportional to $m_{\nu_i}^2$.
2. For $|\Theta_{\ell N}| \gg |\Theta|_{\text{seesaw}}$ (while still keeping neutrino masses small, as experimentally observed) the situation is quite different. The contribution of active neutrinos is negligible, but cancellation between HNL states does occur (similarly to the way it happens in the neutrino mass matrix, see e.g. [108]). On the one hand, the cross-section is always smaller than that of a single HNL with the same mixing. On the other hand, the cross-section can get enhanced as compared to the naive scaling of $\sigma \propto m_\nu^2$ than could have occurred from the Weinberg operator per se (c.f. [74]). This enhancement is roughly by a factor of $|\Theta_{\ell N}|^4/|\Theta|_{\text{seesaw}}^4$ and occurs only if HNLs are sufficiently far from the quasi-Dirac limit (i.e. $m_{N_2}/m_{N_1} = r_N \gtrsim \text{few}$).
3. Lastly, large mass splitting $r_N \gg 1$ does not allow to recover the limit of a single HNL (as considered, e.g. in [73]). Naively, in this case the heavier HNL N_2 and its contribution to $pp \rightarrow \ell^\pm \ell^\pm jj$ should disappear. This is not the case in our realistic (and UV-complete) model (type-I seesaw with 2 HNLs). Indeed, perturbativity demands that all Yukawa couplings are smaller than ~ 1 . For HNLs heavier than the Higgs’s VEV this condition together with the requirement of the smallness of neutrino masses caps not only the value of the mixing angle $|\Theta_{\ell 2}|$ but by extension also $|\Theta_{\ell 1}|$.

As a result, the $pp \rightarrow \ell^\pm \ell^\pm jj$ searches are most sensitive for $r_N \sim \text{few}$ at $m_{N_1} \sim 0.5\text{--}1\text{ TeV}$.¹¹ Even in this case the cross section for the process $pp \rightarrow \ell^\pm \ell^\pm jj$ is about 1 order of magnitude smaller than that of a single HNL with the same mixing angle. At the LHC, the best exclusion limit obtainable in this case would reach $|\Theta_{\ell 1}|^2 \sim 0.02\text{--}0.05$ (assuming background-free search, 100% efficiency of the signal detection and the luminosity of 3 ab^{-1}). In particular, even at the end of the high-luminosity LHC phase (3 ab^{-1} integrated luminosity) these limits are non-competitive with those coming from the *electroweak precision tests* (EWPT) [115] or from non-observations of lepton *flavour violating* process, involving charged leptons [110]. At

¹¹Contribution of the hierarchical HNLs to the $0\nu\beta\beta$ process have been studied recently in [94–96].

the FCC-hh, the exclusion limit could be as low as $|\Theta_{\ell 1}|^2 \sim (2\text{--}5) \times 10^{-4}$ for $r_N \sim \text{few}$ in a mass range of $m_{N_1} \sim \text{few TeV}$. These bounds are competitive with EWPT exclusion. Furthermore, in the regime of $m_{N_1} \sim \text{few TeV}$, they could improve on exclusion bounds set by those of CCDY + $W\gamma$ searches [105].

Throughout this paper we assumed background free searches. This is true only approximately. Indeed, there are Standard Model processes that may lead, e.g. to the appearance of two same-sign W 's in the final states, with subsequent $W \rightarrow \ell\nu$ decays with low missing transverse momentum, see e.g. [49, 116]. Additional sources of the background include: mis-interpretation of jets as leptons (so-called *fake leptons*) [117–119]; processes with 3 or more leptons, some of them escaping the detection; processes with the charge misidentification, etc. At the same time, previous searches [78, 120] show that the backgrounds can indeed be made low by choosing suitable discriminating variables. We leave the detailed studies to the future work. However, we do not expect a drastic change of the results, as further reduction of the signal due to cuts [73] will be in the same ballpark as underestimation of the signal due to the EWA.

In summary: We explored the potential of the WBF signal at the LHC. We concluded that for the planned HL-LHC upgrade it can only contribute meaningful mixing bounds in a quasi-Dirac-like HNL model with HNL mass $m_{N_1} < 1 \text{ TeV}$ and the corresponding mass m_{N_2} according to the mass ratio. For the FCC-hh, the mass range can be extended to $m_{N_1} \sim \text{few TeV}$ yielding competitive limits for mass ratios of $r_N \sim \text{few}$ (see section 2).

The already existing bounds derived from the WBF process [78] can be reinterpreted as bounds on a two HNL model in the highly hierarchical limit owing to the fact that differential cross section for $r_N \gg 1$ looks similar to the single HNL case and therefore the signal acceptance stays roughly the same. We stress again that this does not correspond to a decoupling in the traditional sense, as the “decoupled” and “non-decoupled” HNLs’ mixing angles are explicitly related by the requirement that neutrino masses remain small as observed experimentally.

5.1 Relation between LNV effects and small neutrino masses

Let us comment on the suppression of LNV effects as a consequence of smallness of neutrino masses, a subject of discussion in many works in the past [41, 66, 67, 107, 108, 121]. The relation between the two signals would, essentially, mean that every LNV effective operator [41] is dependent on the Weinberg operator [4]. Our results demonstrate that this is not the case, as even in the qDL model, where neutrino mass is exactly zero, the WBF signal remains finite. We do see, however, that the destructive nature of HNL interference is related to the cancellation of their contributions to the neutrino masses. In the Dirac-limit ($r_N \rightarrow 1$ in our terms), both

the smallness of neutrino masses and LNV collider effects would be proportional to the same small perturbation (e.g. $\Delta M/M$, [107, 108]). However, in the hierarchical case ($r_N > \text{few}$), this does not apply and the two kinds of LNV operators become independent.

The condition $r_N > \text{few}$ implies that our results are not directly applicable to models like the νMSM (where HNLs are highly degenerate [107, 122, 123], see [124] for review). Rather, these results are applicable for leptogenesis models with 3 HNLs [125–127] where the ratio $r_N \sim \text{few}$ and large mixing angles are consistent with successful leptogenesis. We leave the generalisation of our results for the case of 3 HNLs to future works.

The hierarchical HNL spectrum has its own drawbacks. As pointed out in past literature [66, 88, 91, 108, 128–132], the light neutrino mass states generated in models with a highly hierarchical QDL HNL pair can exhibit a significant running of the light masses. This makes these kinds of models theoretically less appealing. Owing to the fact that even hierarchical HNLs are not expected to provide a sizeable signal at the HL-LHC, we leave the detailed exploration of this question to the future.

Acknowledgments

We are grateful to Richard Ruiz and Benjamin Fuks for providing fruitful feedback on the initial version of the manuscript and to Mads T. Frandsen for his valuable input on the JLS.’s Master’s thesis [133]. We would also like to thank Kevin Urquía Calderón, Inar Timiryasov, as well as members of the “NBI HNL group” for many discussions during this work. This project has received funding from the European Research Council (ERC) under the European Union’s Horizon 2020 research and innovation programme (GA 694896) and from the Carlsberg Foundation. O.R. would like to thank the Instituto de Física Teórica (IFT UAM-CSIC) in Madrid for support via the Centro de Excelencia Severo Ochoa Program under Grant CEX2020-001007-S, during the Extended Workshop “Neutrino Theories”, where this work developed.

References

- [1] M. Goeppert-Mayer, *Double beta-disintegration*, *Phys. Rev.* **48** (1935) 512.
- [2] B. Pontecorvo, *Inverse beta-processes and non-conservation of lepton charge*, .
- [3] B. Pontecorvo, *Superweak interactions and double beta decay*, *Phys. Lett. B* **26** (1968) 630.
- [4] S. Weinberg, *Baryon and Lepton Nonconserving Processes*, *Phys. Rev. Lett.* **43** (1979) 1566.

- [5] F. Wilczek and A. Zee, *Operator Analysis of Nucleon Decay*, [*Phys. Rev. Lett.* **43** \(1979\) 1571](#).
- [6] G. Lazarides, Q. Shafi and C. Wetterich, *Proton Lifetime and Fermion Masses in an $SO(10)$ Model*, [*Nucl. Phys. B* **181** \(1981\) 287](#).
- [7] R. N. Mohapatra and J. W. F. Valle, *Neutrino Mass and Baryon Number Nonconservation in Superstring Models*, [*Phys. Rev. D* **34** \(1986\) 1642](#).
- [8] E. Majorana, *Teoria simmetrica dell'elettrone e del positrone*, [*Nuovo Cim.* **14** \(1937\) 171](#).
- [9] S. Dell'Oro, S. Marcocci, M. Viel and F. Vissani, *Neutrinoless double beta decay: 2015 review*, [*Adv. High Energy Phys.* **2016** \(2016\) 2162659 \[1601.07512\]](#).
- [10] V. Cirigliano et al., *Neutrinoless Double-Beta Decay: A Roadmap for Matching Theory to Experiment*, [2203.12169](#).
- [11] SINDRUM II collaboration, J. Kaulard et al., *Improved limit on the branching ratio of $\mu^- \rightarrow e^+$ conversion on titanium*, [*Phys. Lett. B* **422** \(1998\) 334](#).
- [12] BELLE collaboration, Y. Miyazaki et al., *Search for Lepton-Flavor-Violating and Lepton-Number-Violating $\tau \rightarrow lh'h'$ Decay Modes*, [*Phys. Lett. B* **719** \(2013\) 346 \[1206.5595\]](#).
- [13] NA62 collaboration, E. Cortina Gil et al., *Searches for lepton number violating K^+ decays*, [*Phys. Lett. B* **797** \(2019\) 134794 \[1905.07770\]](#).
- [14] BABAR collaboration, J. P. Lees et al., *Search for lepton-number violating processes in $B^+ \rightarrow h^- l^+ l^+$ decays*, [*Phys. Rev. D* **85** \(2012\) 071103 \[1202.3650\]](#).
- [15] LHCb collaboration, R. Aaij et al., *Search for $D^+(s)$ to $\pi^+ \mu^+ \mu^-$ and $D^+(s)$ to $\pi^- \mu^+ \mu^+$ decays*, [*Phys. Lett. B* **724** \(2013\) 203 \[1304.6365\]](#).
- [16] ATLAS collaboration, G. Aad et al., *Inclusive search for same-sign dilepton signatures in pp collisions at $\sqrt{s} = 7$ TeV with the ATLAS detector*, [*JHEP* **10** \(2011\) 107 \[1108.0366\]](#).
- [17] ATLAS collaboration, G. Aad et al., *Search for heavy neutrinos and right-handed W bosons in events with two leptons and jets in pp collisions at $\sqrt{s} = 7$ TeV with the ATLAS detector*, [*Eur. Phys. J. C* **72** \(2012\) 2056 \[1203.5420\]](#).
- [18] CMS collaboration, S. Chatrchyan et al., *Search for heavy Majorana Neutrinos in $\mu^\pm \mu^\pm +$ Jets and $e^\pm e^\pm +$ Jets Events in pp Collisions at $\sqrt{s} = 7$ TeV*, [*Phys. Lett. B* **717** \(2012\) 109 \[1207.6079\]](#).
- [19] ATLAS collaboration, G. Aad et al., *Search for heavy Majorana neutrinos with the ATLAS detector in pp collisions at $\sqrt{s} = 8$ TeV*, [*JHEP* **07** \(2015\) 162 \[1506.06020\]](#).
- [20] CMS collaboration, V. Khachatryan et al., *Search for heavy Majorana neutrinos in $\mu^\pm \mu^\pm +$ jets events in proton-proton collisions at $\sqrt{s} = 8$ TeV*, [*Phys. Lett. B* **748** \(2015\) 144 \[1501.05566\]](#).

- [21] CMS collaboration, V. Khachatryan et al., *Search for heavy Majorana neutrinos in $e^\pm e^\pm + jets$ and $e^\pm \mu^\pm + jets$ events in proton-proton collisions at $\sqrt{s} = 8$ TeV*, *JHEP* **04** (2016) 169 [[1603.02248](#)].
- [22] ATLAS collaboration, M. Aaboud et al., *Search for heavy Majorana or Dirac neutrinos and right-handed W gauge bosons in final states with two charged leptons and two jets at $\sqrt{s} = 13$ TeV with the ATLAS detector*, *JHEP* **01** (2019) 016 [[1809.11105](#)].
- [23] CMS collaboration, A. M. Sirunyan et al., *Search for a heavy right-handed W boson and a heavy neutrino in events with two same-flavor leptons and two jets at $\sqrt{s} = 13$ TeV*, *JHEP* **05** (2018) 148 [[1803.11116](#)].
- [24] CMS collaboration, A. M. Sirunyan et al., *Search for heavy Majorana neutrinos in same-sign dilepton channels in proton-proton collisions at $\sqrt{s} = 13$ TeV*, *JHEP* **01** (2019) 122 [[1806.10905](#)].
- [25] CMS collaboration, A. M. Sirunyan et al., *Search for heavy neutrinos and third-generation leptoquarks in hadronic states of two τ leptons and two jets in proton-proton collisions at $\sqrt{s} = 13$ TeV*, *JHEP* **03** (2019) 170 [[1811.00806](#)].
- [26] LHCb collaboration, R. Aaij et al., *Search for heavy neutral leptons in $W^+ \rightarrow \mu^+ \mu^\pm jet$ decays*, *Eur. Phys. J. C* **81** (2021) 248 [[2011.05263](#)].
- [27] P. Minkowski, *$\mu \rightarrow e\gamma$ at a Rate of One Out of 10^9 Muon Decays?*, *Phys. Lett. B* **67** (1977) 421.
- [28] T. Yanagida, *Horizontal gauge symmetry and masses of neutrinos*, *Conf. Proc. C* **7902131** (1979) 95.
- [29] S. L. Glashow, *The Future of Elementary Particle Physics*, *NATO Sci. Ser. B* **61** (1980) 687.
- [30] M. Gell-Mann, P. Ramond and R. Slansky, *Complex Spinors and Unified Theories*, *Conf. Proc. C* **790927** (1979) 315 [[1306.4669](#)].
- [31] R. N. Mohapatra and G. Senjanovic, *Neutrino Mass and Spontaneous Parity Nonconservation*, *Phys. Rev. Lett.* **44** (1980) 912.
- [32] R. N. Mohapatra and G. Senjanovic, *Neutrino Masses and Mixings in Gauge Models with Spontaneous Parity Violation*, *Phys. Rev. D* **23** (1981) 165.
- [33] J. Schechter and J. W. F. Valle, *Neutrino Masses in $SU(2) \times U(1)$ Theories*, *Phys. Rev. D* **22** (1980) 2227.
- [34] J. Schechter and J. W. F. Valle, *Neutrino Decay and Spontaneous Violation of Lepton Number*, *Phys. Rev. D* **25** (1982) 774.
- [35] I. Esteban, M. C. Gonzalez-Garcia, M. Maltoni, T. Schwetz and A. Zhou, *The fate of hints: updated global analysis of three-flavor neutrino oscillations*, *JHEP* **09** (2020) 178 [[2007.14792](#)].

- [36] C. Dvorkin et al., *Neutrino Mass from Cosmology: Probing Physics Beyond the Standard Model*, [1903.03689](#).
- [37] D. A. Dicus, D. D. Karatas and P. Roy, *Lepton nonconservation at supercollider energies*, *Phys. Rev. D* **44** (1991) 2033.
- [38] A. Datta, M. Guchait and A. Pilaftsis, *Probing lepton number violation via majorana neutrinos at hadron supercolliders*, *Phys. Rev. D* **50** (1994) 3195 [[hep-ph/9311257](#)].
- [39] A. Ali, A. V. Borisov and N. B. Zamorin, *Majorana neutrinos and same sign dilepton production at LHC and in rare meson decays*, *Eur. Phys. J. C* **21** (2001) 123 [[hep-ph/0104123](#)].
- [40] O. Panella, M. Cannoni, C. Carimalo and Y. N. Srivastava, *Signals of heavy Majorana neutrinos at hadron colliders*, *Phys. Rev. D* **65** (2002) 035005 [[hep-ph/0107308](#)].
- [41] A. de Gouvea and J. Jenkins, *A Survey of Lepton Number Violation Via Effective Operators*, *Phys. Rev. D* **77** (2008) 013008 [[0708.1344](#)].
- [42] F. del Aguila and J. A. Aguilar-Saavedra, *$l W \nu$ production at CLIC: A Window to TeV scale non-decoupled neutrinos*, *JHEP* **05** (2005) 026 [[hep-ph/0503026](#)].
- [43] F. del Aguila, J. A. Aguilar-Saavedra and R. Pittau, *Neutrino physics at large colliders*, *J. Phys. Conf. Ser.* **53** (2006) 506 [[hep-ph/0606198](#)].
- [44] T. Han and B. Zhang, *Signatures for Majorana neutrinos at hadron colliders*, *Phys. Rev. Lett.* **97** (2006) 171804 [[hep-ph/0604064](#)].
- [45] F. del Aguila and J. A. Aguilar-Saavedra, *Like-sign dilepton signals from a leptophobic Z' boson*, *JHEP* **11** (2007) 072 [[0705.4117](#)].
- [46] C.-S. Chen, C.-Q. Geng and D. V. Zhuridov, *Same-sign single dilepton productions at the LHC*, *Phys. Lett. B* **666** (2008) 340 [[0801.2011](#)].
- [47] P. Fileviez Perez, T. Han, G.-Y. Huang, T. Li and K. Wang, *Testing a Neutrino Mass Generation Mechanism at the LHC*, *Phys. Rev. D* **78** (2008) 071301 [[0803.3450](#)].
- [48] W. Chao, Z.-g. Si, Y.-j. Zheng and S. Zhou, *Testing the Realistic Seesaw Model with Two Heavy Majorana Neutrinos at the CERN Large Hadron Collider*, *Phys. Lett. B* **683** (2010) 26 [[0907.0935](#)].
- [49] M. T. Frandsen, I. Masina and F. Sannino, *Fourth Lepton Family is Natural in Technicolor*, *Phys. Rev. D* **81** (2010) 035010 [[0905.1331](#)].
- [50] G. Altarelli and F. Feruglio, *Discrete Flavor Symmetries and Models of Neutrino Mixing*, *Rev. Mod. Phys.* **82** (2010) 2701 [[1002.0211](#)].
- [51] A. Ibarra, E. Molinaro and S. T. Petcov, *Low Energy Signatures of the TeV Scale See-Saw Mechanism*, *Phys. Rev. D* **84** (2011) 013005 [[1103.6217](#)].

- [52] T. Han, I. Lewis, R. Ruiz and Z.-g. Si, *Lepton Number Violation and W' Chiral Couplings at the LHC*, *Phys. Rev. D* **87** (2013) 035011 [[1211.6447](#)].
- [53] P. W. Angel, N. L. Rodd and R. R. Volkas, *Origin of neutrino masses at the LHC: $\Delta L = 2$ effective operators and their ultraviolet completions*, *Phys. Rev. D* **87** (2013) 073007 [[1212.6111](#)].
- [54] J. C. Helo, M. Hirsch, H. Päs and S. G. Kovalenko, *Short-range mechanisms of neutrinoless double beta decay at the LHC*, *Phys. Rev. D* **88** (2013) 073011 [[1307.4849](#)].
- [55] J. C. Helo, M. Hirsch, S. G. Kovalenko and H. Pas, *Neutrinoless double beta decay and lepton number violation at the LHC*, *Phys. Rev. D* **88** (2013) 011901 [[1303.0899](#)].
- [56] A. de Gouvea and P. Vogel, *Lepton Flavor and Number Conservation, and Physics Beyond the Standard Model*, *Prog. Part. Nucl. Phys.* **71** (2013) 75 [[1303.4097](#)].
- [57] S. F. King, A. Merle, S. Morisi, Y. Shimizu and M. Tanimoto, *Neutrino Mass and Mixing: from Theory to Experiment*, *New J. Phys.* **16** (2014) 045018 [[1402.4271](#)].
- [58] F. F. Deppisch, P. S. Bhupal Dev and A. Pilaftsis, *Neutrinos and Collider Physics*, *New J. Phys.* **17** (2015) 075019 [[1502.06541](#)].
- [59] J. N. Ng, A. de la Puente and B. W.-P. Pan, *Search for Heavy Right-Handed Neutrinos at the LHC and Beyond in the Same-Sign Same-Flavor Leptons Final State*, *JHEP* **12** (2015) 172 [[1505.01934](#)].
- [60] A. Das, P. Konar and S. Majhi, *Production of Heavy neutrino in next-to-leading order QCD at the LHC and beyond*, *JHEP* **06** (2016) 019 [[1604.00608](#)].
- [61] G. Anamiati, M. Hirsch and E. Nardi, *Quasi-Dirac neutrinos at the LHC*, *JHEP* **10** (2016) 010 [[1607.05641](#)].
- [62] A. Das and N. Okada, *Bounds on heavy Majorana neutrinos in type-I seesaw and implications for collider searches*, *Phys. Lett. B* **774** (2017) 32 [[1702.04668](#)].
- [63] A. Abada, V. De Romeri, M. Lucente, A. M. Teixeira and T. Toma, *Effective Majorana mass matrix from tau and pseudoscalar meson lepton number violating decays*, *JHEP* **02** (2018) 169 [[1712.03984](#)].
- [64] Y. Cai, T. Han, T. Li and R. Ruiz, *Lepton Number Violation: Seesaw Models and Their Collider Tests*, *Front. in Phys.* **6** (2018) 40 [[1711.02180](#)].
- [65] E. J. Chun, A. Das, S. Mandal, M. Mitra and N. Sinha, *Sensitivity of Lepton Number Violating Meson Decays in Different Experiments*, *Phys. Rev. D* **100** (2019) 095022 [[1908.09562](#)].
- [66] M. Drewes, J. Klarić and P. Klose, *On lepton number violation in heavy neutrino decays at colliders*, *JHEP* **11** (2019) 032 [[1907.13034](#)].
- [67] J.-L. Tastet and I. Timiryasov, *Dirac vs. Majorana HNLs (and their oscillations) at SHiP*, *JHEP* **04** (2020) 005 [[1912.05520](#)].

- [68] J. De Vries, H. K. Dreiner, J. Y. Günther, Z. S. Wang and G. Zhou, *Long-lived Sterile Neutrinos at the LHC in Effective Field Theory*, *JHEP* **03** (2021) 148 [[2010.07305](#)].
- [69] J. Gargalionis and R. R. Volkas, *Exploding operators for Majorana neutrino masses and beyond*, *JHEP* **01** (2021) 074 [[2009.13537](#)].
- [70] A. de Gouvêa, P. J. Fox, B. J. Kayser and K. J. Kelly, *Characterizing heavy neutral fermions via their decays*, *Phys. Rev. D* **105** (2022) 015019 [[2109.10358](#)].
- [71] G. Zhou, *Light sterile neutrinos and lepton-number-violating kaon decays in effective field theory*, *JHEP* **06** (2022) 127 [[2112.00767](#)].
- [72] M. Aoki, K. Enomoto and S. Kanemura, *Probing charged lepton number violation via $\ell^\pm \ell'^\pm W^\mp W^\mp$* , *Phys. Rev. D* **101** (2020) 115019 [[2002.12265](#)].
- [73] B. Fuks, J. Neundorff, K. Peters, R. Ruiz and M. Saimpert, *Majorana neutrinos in same-sign $W^\pm W^\pm$ scattering at the LHC: Breaking the TeV barrier*, *Phys. Rev. D* **103** (2021) 055005 [[2011.02547](#)].
- [74] B. Fuks, J. Neundorff, K. Peters, R. Ruiz and M. Saimpert, *Probing the Weinberg operator at colliders*, *Phys. Rev. D* **103** (2021) 115014 [[2012.09882](#)].
- [75] G. Zapata, T. Urruzola, O. A. Sampayo and L. Duarte, *Lepton collider probes for Majorana neutrino effective interactions*, *Eur. Phys. J. C* **82** (2022) 544 [[2201.02480](#)].
- [76] F. del Aguila, J. A. Aguilar-Saavedra and R. Pittau, *Heavy neutrino signals at large hadron colliders*, *JHEP* **10** (2007) 047 [[hep-ph/0703261](#)].
- [77] C. Degrande, O. Mattelaer, R. Ruiz and J. Turner, *Fully-Automated Precision Predictions for Heavy Neutrino Production Mechanisms at Hadron Colliders*, *Phys. Rev. D* **94** (2016) 053002 [[1602.06957](#)].
- [78] CMS collaboration, *Probing heavy Majorana neutrinos and the Weinberg operator through vector boson fusion processes in proton-proton collisions at $\sqrt{s} = 13$ TeV*, [2206.08956](#).
- [79] R. N. Mohapatra, *Mechanism for Understanding Small Neutrino Mass in Superstring Theories*, *Phys. Rev. Lett.* **56** (1986) 561.
- [80] J. Bernabeu, A. Santamaria, J. Vidal, A. Mendez and J. W. F. Valle, *Lepton Flavor Nonconservation at High-Energies in a Superstring Inspired Standard Model*, *Phys. Lett. B* **187** (1987) 303.
- [81] E. K. Akhmedov, M. Lindner, E. Schnapka and J. W. F. Valle, *Left-right symmetry breaking in NJL approach*, *Phys. Lett. B* **368** (1996) 270 [[hep-ph/9507275](#)].
- [82] E. K. Akhmedov, M. Lindner, E. Schnapka and J. W. F. Valle, *Dynamical left-right symmetry breaking*, *Phys. Rev. D* **53** (1996) 2752 [[hep-ph/9509255](#)].
- [83] A. Halprin, S. T. Petcov and S. P. Rosen, *Effects of Light and Heavy Majorana Neutrinos in Neutrinoless Double Beta Decay*, *Phys. Lett. B* **125** (1983) 335.

- [84] P. Benes, A. Faessler, F. Simkovic and S. Kovalenko, *Sterile neutrinos in neutrinoless double beta decay*, *Phys. Rev. D* **71** (2005) 077901 [[hep-ph/0501295](#)].
- [85] F. L. Bezrukov, *nu MSM-predictions for neutrinoless double beta decay*, *Phys. Rev. D* **72** (2005) 071303 [[hep-ph/0505247](#)].
- [86] M. Blennow, E. Fernandez-Martinez, J. Lopez-Pavon and J. Menendez, *Neutrinoless double beta decay in seesaw models*, *JHEP* **07** (2010) 096 [[1005.3240](#)].
- [87] M. Mitra, G. Senjanovic and F. Vissani, *Neutrinoless Double Beta Decay and Heavy Sterile Neutrinos*, *Nucl. Phys. B* **856** (2012) 26 [[1108.0004](#)].
- [88] J. Lopez-Pavon, S. Pascoli and C.-f. Wong, *Can heavy neutrinos dominate neutrinoless double beta decay?*, *Phys. Rev. D* **87** (2013) 093007 [[1209.5342](#)].
- [89] T. Asaka and S. Eijima, *Direct Search for Right-handed Neutrinos and Neutrinoless Double Beta Decay*, *PTEP* **2013** (2013) 113B02 [[1308.3550](#)].
- [90] A. Faessler, M. González, S. Kovalenko and F. Šimkovic, *Arbitrary mass Majorana neutrinos in neutrinoless double beta decay*, *Phys. Rev. D* **90** (2014) 096010 [[1408.6077](#)].
- [91] J. Lopez-Pavon, E. Molinaro and S. T. Petcov, *Radiative Corrections to Light Neutrino Masses in Low Scale Type I Seesaw Scenarios and Neutrinoless Double Beta Decay*, *JHEP* **11** (2015) 030 [[1506.05296](#)].
- [92] P. Hernández, M. Kekic, J. López-Pavón, J. Racker and J. Salvado, *Testable Baryogenesis in Seesaw Models*, *JHEP* **08** (2016) 157 [[1606.06719](#)].
- [93] M. Drewes and S. Eijima, *Neutrinoless double β decay and low scale leptogenesis*, *Phys. Lett. B* **763** (2016) 72 [[1606.06221](#)].
- [94] T. Asaka, H. Ishida and K. Tanaka, *What if a specific neutrinoless double beta decay is absent?*, *PTEP* **2021** (2021) 063B01 [[2012.13186](#)].
- [95] T. Asaka, H. Ishida and K. Tanaka, *Hiding neutrinoless double beta decay in the minimal seesaw mechanism*, *Phys. Rev. D* **103** (2021) 015014 [[2012.12564](#)].
- [96] T. Asaka, H. Ishida and K. Tanaka, *Neutrinoless double beta decays tell nature of right-handed neutrinos*, [2101.12498](#).
- [97] A. Ibarra, E. Molinaro and S. T. Petcov, *TeV Scale See-Saw Mechanisms of Neutrino Mass Generation, the Majorana Nature of the Heavy Singlet Neutrinos and $(\beta\beta)_{0\nu}$ -Decay*, *JHEP* **09** (2010) 108 [[1007.2378](#)].
- [98] S. Dawson, *The Effective W Approximation*, *Nucl. Phys. B* **249** (1985) 42.
- [99] G. L. Kane, W. W. Repko and W. B. Rolnick, *The Effective W_{+-} , $Z0$ Approximation for High-Energy Collisions*, *Phys. Lett. B* **148** (1984) 367.
- [100] Z. Kunszt and D. E. Soper, *On the Validity of the Effective W Approximation*, *Nucl. Phys. B* **296** (1988) 253.
- [101] R. Ruiz, A. Costantini, F. Maltoni and O. Mattelaer, *The Effective Vector Boson Approximation in high-energy muon collisions*, *JHEP* **06** (2022) 114 [[2111.02442](#)].

- [102] R. E. Ruiz, *Hadron Collider Tests of Neutrino Mass-Generating Mechanisms*, Ph.D. thesis, Pittsburgh U., 2015. [1509.06375](#).
- [103] CMS COLLABORATION collaboration, A. M. Sirunyan, A. Tumasyan, W. Adam, F. Ambrogi, E. Asilar, T. Bergauer et al., *Search for heavy neutral leptons in events with three charged leptons in proton-proton collisions at $\sqrt{s} = 13$ TeV*, *Phys. Rev. Lett.* **120** (2018) 221801.
- [104] D. Alva, T. Han and R. Ruiz, *Heavy Majorana neutrinos from $W\gamma$ fusion at hadron colliders*, *JHEP* **02** (2015) 072 [[1411.7305](#)].
- [105] S. Pascoli, R. Ruiz and C. Weiland, *Heavy neutrinos with dynamic jet vetoes: multilepton searches at $\sqrt{s} = 14, 27, \text{ and } 100$ TeV*, *JHEP* **06** (2019) 049 [[1812.08750](#)].
- [106] A. Denner, H. Eck, O. Hahn and J. Kublbeck, *Feynman rules for fermion number violating interactions*, *Nucl. Phys. B* **387** (1992) 467.
- [107] M. Shaposhnikov, *A Possible symmetry of the nuMSM*, *Nucl. Phys. B* **763** (2007) 49 [[hep-ph/0605047](#)].
- [108] J. Kersten and A. Y. Smirnov, *Right-Handed Neutrinos at CERN LHC and the Mechanism of Neutrino Mass Generation*, *Phys. Rev. D* **76** (2007) 073005 [[0705.3221](#)].
- [109] T. Appelquist and J. Carazzone, *Infrared Singularities and Massive Fields*, *Phys. Rev. D* **11** (1975) 2856.
- [110] K. A. Urquía Calderón, I. Timiryasov and O. Ruchayskiy, *Improved constraints and the prospects of detecting TeV to PeV scale Heavy Neutral Leptons*, [2206.04540](#).
- [111] O. Aberle et al., *High-Luminosity Large Hadron Collider (HL-LHC): Technical design report*, CERN Yellow Reports: Monographs. CERN, Geneva, 2020, [10.23731/CYRM-2020-0010](#).
- [112] FCC collaboration, A. Abada et al., *FCC Physics Opportunities: Future Circular Collider Conceptual Design Report Volume 1*, *Eur. Phys. J. C* **79** (2019) 474.
- [113] M. Aleksa et al., *Calorimeters for the FCC-hh*, [1912.09962](#).
- [114] A. Ali, A. V. Borisov and N. B. Zamorin, *Same-sign Dilepton Production via Heavy Majorana Neutrinos in Proton-proton Collisions*, in *10th Lomonosov Conference on Elementary Particle Physics*, pp. 74–79, 2003, [hep-ph/0112043](#), DOI.
- [115] E. Fernandez-Martinez, J. Hernandez-Garcia and J. Lopez-Pavon, *Global constraints on heavy neutrino mixing*, *JHEP* **08** (2016) 033 [[1605.08774](#)].
- [116] A. Alboteanu, W. Kilian and J. Reuter, *Resonances and Unitarity in Weak Boson Scattering at the LHC*, *JHEP* **11** (2008) 010 [[0806.4145](#)].
- [117] ATLAS collaboration, *Data-Quality Requirements and Event Cleaning for Jets and Missing Transverse Energy Reconstruction with the ATLAS Detector in*

Proton-Proton Collisions at a Center-of-Mass Energy of $\sqrt{s} = 7$ TeV, tech. rep., 7, 2010.

- [118] ATLAS collaboration, *Estimation of non-prompt and fake lepton backgrounds in final states with top quarks produced in proton-proton collisions at $\sqrt{s} = 8$ TeV with the ATLAS detector*, tech. rep., 10, 2014.
- [119] X. Thusini, *Characterising the sources of fake leptons from top quarks in same sign W boson scattering with the ATLAS detector at $\sqrt{s} = 13$ TeV*, Master's thesis, Cape Town U., 2017.
- [120] CMS collaboration, S. Chatrchyan et al., *Search for new physics in events with same-sign dileptons and b -tagged jets in pp collisions at $\sqrt{s} = 7$ TeV*, *JHEP* **08** (2012) 110 [[1205.3933](#)].
- [121] K. Moffat, S. Pascoli and C. Weiland, *Equivalence between massless neutrinos and lepton number conservation in fermionic singlet extensions of the Standard Model*, [1712.07611](#).
- [122] T. Asaka and M. Shaposhnikov, *The ν MSM, dark matter and baryon asymmetry of the universe*, *Phys. Lett. B* **620** (2005) 17 [[hep-ph/0505013](#)].
- [123] T. Asaka, S. Blanchet and M. Shaposhnikov, *The ν MSM, dark matter and neutrino masses*, *Phys. Lett. B* **631** (2005) 151 [[hep-ph/0503065](#)].
- [124] A. Boyarsky, O. Ruchayskiy and M. Shaposhnikov, *The Role of sterile neutrinos in cosmology and astrophysics*, *Ann. Rev. Nucl. Part. Sci.* **59** (2009) 191 [[0901.0011](#)].
- [125] E. K. Akhmedov, V. A. Rubakov and A. Y. Smirnov, *Baryogenesis via Neutrino Oscillations*, *Phys. Rev. Lett.* **81** (1998) 1359 [[hep-ph/9803255](#)].
- [126] M. Drewes, B. Garbrecht, P. Hernandez, M. Kekic, J. Lopez-Pavon, J. Racker et al., *ARS Leptogenesis*, *Int. J. Mod. Phys. A* **33** (2018) 1842002 [[1711.02862](#)].
- [127] A. Abada, G. Arcadi, V. Domcke, M. Drewes, J. Klaric and M. Lucente, *Low-scale leptogenesis with three heavy neutrinos*, *JHEP* **01** (2019) 164 [[1810.12463](#)].
- [128] A. Pilaftsis, *Radiatively induced neutrino masses and large Higgs neutrino couplings in the standard model with Majorana fields*, *Z. Phys. C* **55** (1992) 275 [[hep-ph/9901206](#)].
- [129] J. G. Korner, A. Pilaftsis and K. Schilcher, *Leptonic CP asymmetries in flavor changing H^0 decays*, *Phys. Rev. D* **47** (1993) 1080 [[hep-ph/9301289](#)].
- [130] D. Aristizabal Sierra and C. E. Yaguna, *On the importance of the 1-loop finite corrections to seesaw neutrino masses*, *JHEP* **08** (2011) 013 [[1106.3587](#)].
- [131] S. Pascoli, M. Mitra and S. Wong, *Effect of cancellation in neutrinoless double beta decay*, *Phys. Rev. D* **90** (2014) 093005 [[1310.6218](#)].
- [132] N. Haba, H. Ishida and Y. Yamaguchi, *Naturalness and lepton number/flavor violation in inverse seesaw models*, *JHEP* **11** (2016) 003 [[1608.07447](#)].

- [133] J. Schubert, *Interference Between Majorana States in the “Neutrinoless Double Beta Decay” at Colliders. Phenomenology of Heavy Neutral Lepton*, Master’s thesis, University of Copenhagen, September, 2022.
- [134] S. Alekhin et al., *A facility to Search for Hidden Particles at the CERN SPS: the SHiP physics case*, *Rept. Prog. Phys.* **79** (2016) 124201 [[1504.04855](#)].
- [135] A. M. Abdullahi et al., *The Present and Future Status of Heavy Neutral Leptons*, in *2022 Snowmass Summer Study*, 3, 2022, [2203.08039](#).
- [136] M. S. Chanowitz, M. A. Furman and I. Hinchliffe, *Weak Interactions of Ultraheavy Fermions. 2.*, *Nucl. Phys. B* **153** (1979) 402.
- [137] L. Durand, J. M. Johnson and J. L. Lopez, *Perturbative Unitarity Revisited: A New Upper Bound on the Higgs Boson Mass*, *Phys. Rev. Lett.* **64** (1990) 1215.
- [138] S. Fajfer and A. Ilakovac, *Lepton flavor violation in light hadron decays*, *Phys. Rev. D* **57** (1998) 4219.
- [139] S. Ipek, A. D. Plascencia and J. Turner, *Assessing Perturbativity and Vacuum Stability in High-Scale Leptogenesis*, *JHEP* **12** (2018) 111 [[1806.00460](#)].
- [140] M. Drewes, *On the Minimal Mixing of Heavy Neutrinos*, [1904.11959](#).
- [141] M. Aker, A. Beglarian, J. Behrens, A. Berlev, U. Besserer, B. Bieringer et al., *Direct neutrino-mass measurement with sub-electronvolt sensitivity*, *Nature Physics* **18** (2022) 160.
- [142] A. D. Martin, W. J. Stirling, R. S. Thorne and G. Watt, *Parton distributions for the LHC*, *The European Physical Journal C* **63** (2009) 189.

A Type I seesaw

In this section we summarise the main formulas of the type-I seesaw model with the goal to fix the notations. For references see, e.g. [[134](#), [135](#)] and refs. therein.

Before Electro-Weak Symmetry Breaking (EWSB) the type-I seesaw Lagrangian is

$$\mathcal{L}_{\text{seesaw}} = \mathcal{L}_{\text{SM}} + \frac{i}{2} \nu_{RI}^\dagger \bar{\sigma}^\mu \partial_\mu \nu_{RI} - (F_{\alpha I})^* \left(L_\alpha \cdot \tilde{\phi} \right)^\dagger \nu_{RI} - \frac{M_I}{2} \nu_{RI}^T \nu_{RI} + h.c. \quad (\text{A.1})$$

Here ν_{RI} are the new right-chiral singlet states with $I = 1, \dots, \mathcal{N}$ with associated Majorana masses M_I , L_α is the SM left chiral SU(2) doublet $L_\alpha = \begin{pmatrix} \nu_\alpha \\ l_\alpha \end{pmatrix}_L$, where $\alpha = e, \mu, \tau$ and $\tilde{\phi}_\alpha = \varepsilon_{ab} \phi_b^*$, where ϕ is the Higgs doublet. After EWSB, this can be written as $\phi = \frac{1}{\sqrt{2}} \begin{pmatrix} 0 \\ v \end{pmatrix}$, where v is the vacuum expectation value (VEV). And so

$(L_\alpha \cdot \tilde{\phi}) = \frac{v}{\sqrt{2}} \nu_{L\alpha}$ after EWSB. The terms

$$\mathcal{L}_D = - (F_{\alpha I}^\nu)^* \frac{v}{\sqrt{2}} \nu_{L\alpha}^\dagger \nu_{RI} + h.c. \quad (\text{A.2})$$

are equivalent to Dirac mass terms with $(m_D)_{\alpha I} = \frac{v}{\sqrt{2}} (F_{\alpha I}^\nu)^*$. Diagonalising the mass term leads to two types of Majorana states: \mathcal{N} heavy Majorana states N_I with masses

$$m_{N_I} \simeq M_I \quad (\text{A.3})$$

and three light Majorana neutrinos whose masses are given by the *seesaw formula*

$$\left(V^\dagger \text{diag}(m_{\nu_1}, m_{\nu_2}, m_{\nu_3}) V \right)_{\alpha\beta} \simeq \sum_I \Theta_{\alpha I} \Theta_{\beta I} m_{N_I}. \quad (\text{A.4})$$

Here $V_{i\alpha}$ is the PMNS matrix, while $\Theta_{\alpha I}$ are the active-sterile mixing angles¹²

$$\Theta_{\alpha I} \equiv \frac{F_{\alpha I}^\nu v}{M_I}. \quad (\text{A.5})$$

The Majorana scale is not fixed and can range from $\sim \text{eV}$ to 10^{15} GeV .

A.1 Perturbativity limit

The seesaw relation in eq. (A.4) is derived under the assumption

$$\text{Type-I seesaw: } |\Theta_{\alpha I}| < 1. \quad (\text{A.6})$$

However, for large HNL masses, $m_{N_I} \gtrsim v$, the requirement of perturbativity of the model described by eq. (A.1), $|F_{\alpha I}^\nu| < 1$ becomes more restrictive than eq. (A.6) (see also [110, 136–139] for the discussion of perturbativity in the Type I seesaw model). Indeed, owing to eq. (A.5) we get

$$\text{Perturbativity: } |\Theta_{\alpha I}| < \frac{v}{M_I}. \quad (\text{A.7})$$

The conditions in eqs. (A.6) and (A.7) were used in section 4 when deriving maximal number of events produced at colliders figure 7.¹³ Owing to the extra loop factor $\frac{1}{(4\pi)^2}$ the perturbativity limit (A.7) can be pushed up by a factor of 4π .

Finally, it should be noted that a type-I seesaw model produces light neutrino masses of the order $m \sim |\Theta|^2 m_{N_1}$. This defines a minimal mixing angle, admissible for a given HNL mass, commonly referred to as the *seesaw line*

$$|\Theta|_{\text{seesaw}}^2 = \frac{\sqrt{|\Delta m_{\text{atm}}^2|}}{m_N}. \quad (\text{A.8})$$

¹²To make the notation more readable, we will sometimes write $\Theta_{\ell N}$ instead of $\Theta_{\alpha I}$.

¹³Notice that in a model as described in section 3, this requirement will be imposed on the heavier of the two HNLs and entail a limit on $\Theta_{\ell 1}$ through eq. (3.2).

B Single HNL Case – Seesaw Line

In a toy model including only 1 HNL, the smallness of the light neutrino mass states can only be introduced by a sufficiently small mixing $\Theta_{\alpha N}$. This model can not account for neutrino oscillations, since it can maximally generate a single potentially degenerate, non-zero, light mass state level [140]. For demonstration purposes, we will only consider a single non-zero light state with a PMNS-like mixing of 1. We will further generously set the value of the light neutrino mass to 1 eV, which roughly corresponds to the current direct upper bound on neutrino masses [141]. To this effect, we consider a mixing $|\Theta_{\ell N}^2| = 1 \text{ eV}/m_N$, which yields a constant light mass state for a given m_N according to eq. (2.5).

Averaging over W polarisations contracted with the amplitude in eq. (2.3) we find the differential cross section of the $W^\pm W^\pm \rightarrow \ell^\pm \ell^\pm$ process considering both heavy and light states. This is shown for an HNL mass of 150 GeV as the blue graph in figure 12. Similarly, we can derive the differential cross section if only light (shown in dash-dotted green) or heavy (dashed orange) mass states contributed to the process. It's important to note that the isolated light mass state case yields a larger differential cross section than both the isolated heavy case and the combined case. This is true over the entire t range, while at the extremal values the isolated N-case drops slightly and the combined case approaches the ν -case. That is to say, the isolated heavy case results in a relatively even angular distribution, while the light case strongly favours back-to-back scattering. Due to the cancelling nature of the two contributions, which is the strongest while both u and t are large when compared to m_N^2 , the combined differential cross section has an even stronger tendency toward back-to-back scattering.

Integrating the differential cross section with respect to t we find the total cross section, shown in figure 13. As prescribed by the mixing angle, the isolated light mass state case (again in dash-dotted green) results in a constant cross section with respect to m_N . As expected from the differential cross section the light line represents an upper limit to the numerical value of the combined cross section (solid blue). For small HNL masses ($m_N^2 \lesssim |t|_{\min}$) both heavy and light mass states will have a near identical differential cross section, leading to a vanishing combined cross section. For large HNL masses ($m_N^2 \gtrsim |t|_{\max}$) the denominator of the HNL propagator is always dominated by the mass term. This, combined with the mixing prescription, results in the cross section of the heavy case dropping as m_N^{-4} , and the combined cross section asymptotically approaching the light line.

We would like to draw attention to the fact that the numerical values of the cross section resulting in this model are vanishingly small. Consequently, even given the uniqueness of the signature, there would be no hope of detection of a process involving

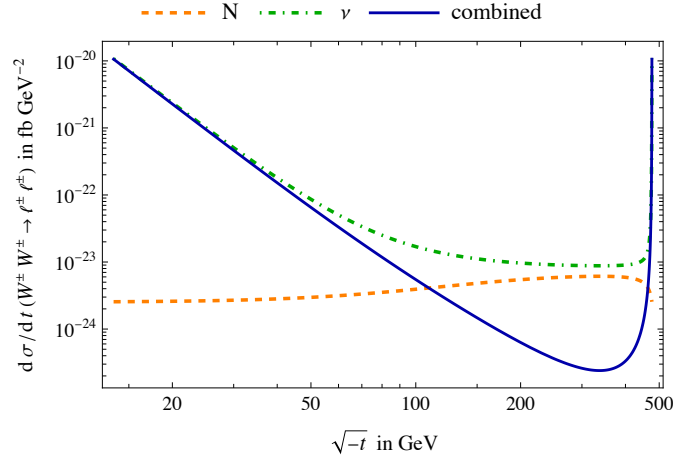


Figure 12: Differential cross section of $W^\pm W^\pm \rightarrow \ell^\pm \ell^\pm$ scattering in the case of a single HNL with mass $m_N = 150$ GeV as a function the Mandelstam-variable t at a centre of mass energy of 500 GeV. The mixing angle here is a function of the HNL mass, such that $|\Theta_{\ell N}^2 m_N| = 1 \text{ eV} \gtrsim m_{\nu_e}$. For further information see text.

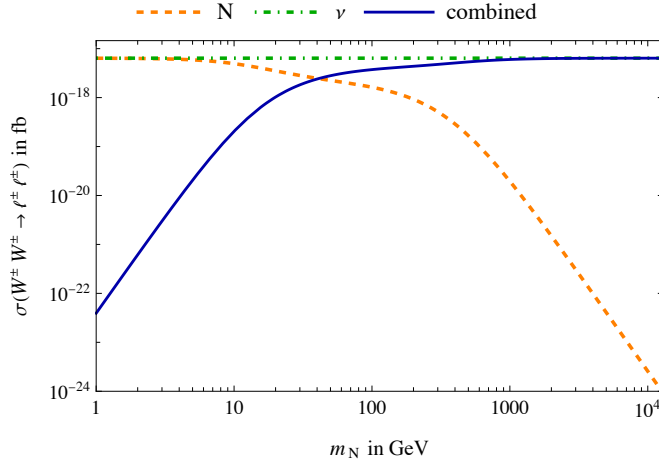


Figure 13: Cross section of $W^\pm W^\pm \rightarrow \ell^\pm \ell^\pm$ scattering in the case of a single HNL as a function of the HNL mass at a centre of mass energy of 500 GeV. The mixing angle here is a function of the HNL mass as well, such that $|\Theta_{\ell N}^2 m_N| = 1 \text{ eV} \gtrsim m_{\nu_e}$. For further information see text.

$W^\pm W^\pm \rightarrow \ell^\pm \ell^\pm$ in terms of a single HNL model.

C Realistic model with two HNLs plus light Majorana states

Given the importance of the light mass states in the single HNL case, it is prudent to investigate their relevance when it comes to the two HNL case as well. An easy way

to incorporate them into the model is by using the Casas-Ibarra parametrisation of the mixing angles

$$\Theta = iU \text{diag}(m_{\nu_1}, m_{\nu_2}, m_{\nu_3})^{1/2} \Omega \text{diag}(m_{N_1}, \dots, m_{N_{\mathcal{N}}})^{-1/2}, \quad (\text{C.1})$$

which, by design, generates the light mass states m_{ν_i} through eq. (2.5). Here Ω is an orthogonal $3 \times \mathcal{N}$ matrix holding all degrees of freedom of the model that aren't fixed by the PMNS matrix U , and the mass states m_{ν_i} , and m_{N_I} . To account for neutrino oscillations with 2 HNLs, we require the lightest neutrino mass state to be massless. The most general explicit form of Ω in case of normal hierarchy (NH) is given by

$$\Omega = \begin{pmatrix} 0 & 0 \\ \cos \omega & \sin \omega \\ -\xi \sin \omega & \xi \cos \omega \end{pmatrix}, \quad (\text{C.2})$$

with $\xi = \pm 1$, and $\omega \in \mathbb{C}$. The parity ξ can be chosen by simultaneous redefinition of the fields and ω so that we will choose $\xi = +1$ without loss of generality. In the following we present the numerical values for the case of normal hierarchy with $\ell = e$.¹⁴ The real part of the Casas-Ibarra parameter ω only regulates which PMNS entry talks to which HNL, while $\text{Im}(\omega)$ determines the absolute scale of the mixing angle.

Figure 14 shows the differential cross section in a model with two non-zero light and two heavy mass states for $\omega = 0$ (no enhancement), $\omega = 5i$ (moderate enhancement), and $\omega = 15i$ (strong enhancement) respectively. Here, the two HNL curves are both given for a mass m_{N_1} but represent the two possible mixing angles of the Casas-Ibarra parametrisation determined by $\text{Re}(\omega)$. We see that, in the case of no enhancement, the situation is rather similar to the single HNL case (figure 12), where the differential cross section is dominated by the light states, and we get a strong back-to-back scattering. The strongly enhanced case is essentially the same as the quasi-Dirac-like model of two HNLs (figure 4), but with a mixing angle slightly smaller than 1.¹⁵ For large r_N , the moderately enhanced case exhibits the same characteristics as the strongly enhanced case. However, for smaller r_N the combined cross section becomes comparable to that of the isolated light mass states, so that non-trivial cancellations occur.

Figure 15 compares the $W^\pm W^\pm \rightarrow \ell^\pm \ell^\pm$ cross section as evaluated in a fully realistic 2 HNL model with the same in the QDL approximation. We see that for a maximal theoretically admissible mixing angle there is no observable difference between the two results at the scales presented here.¹⁶

¹⁴The results will be equivalent for other choices up to orders of few in PMNS matrix entry ratios.

¹⁵Indeed, it is directly comparable with QDL with a mixing angle of $\Theta_{\ell 1}^{\text{QDL}} = |\Theta_{\ell 1}^{\text{CI}}(\omega = 15i)| < 1$ (see also figure 15).

¹⁶As described in section 4, this means that the mixing angle fully satisfies either the Seesaw or Yukawa expansion limit.

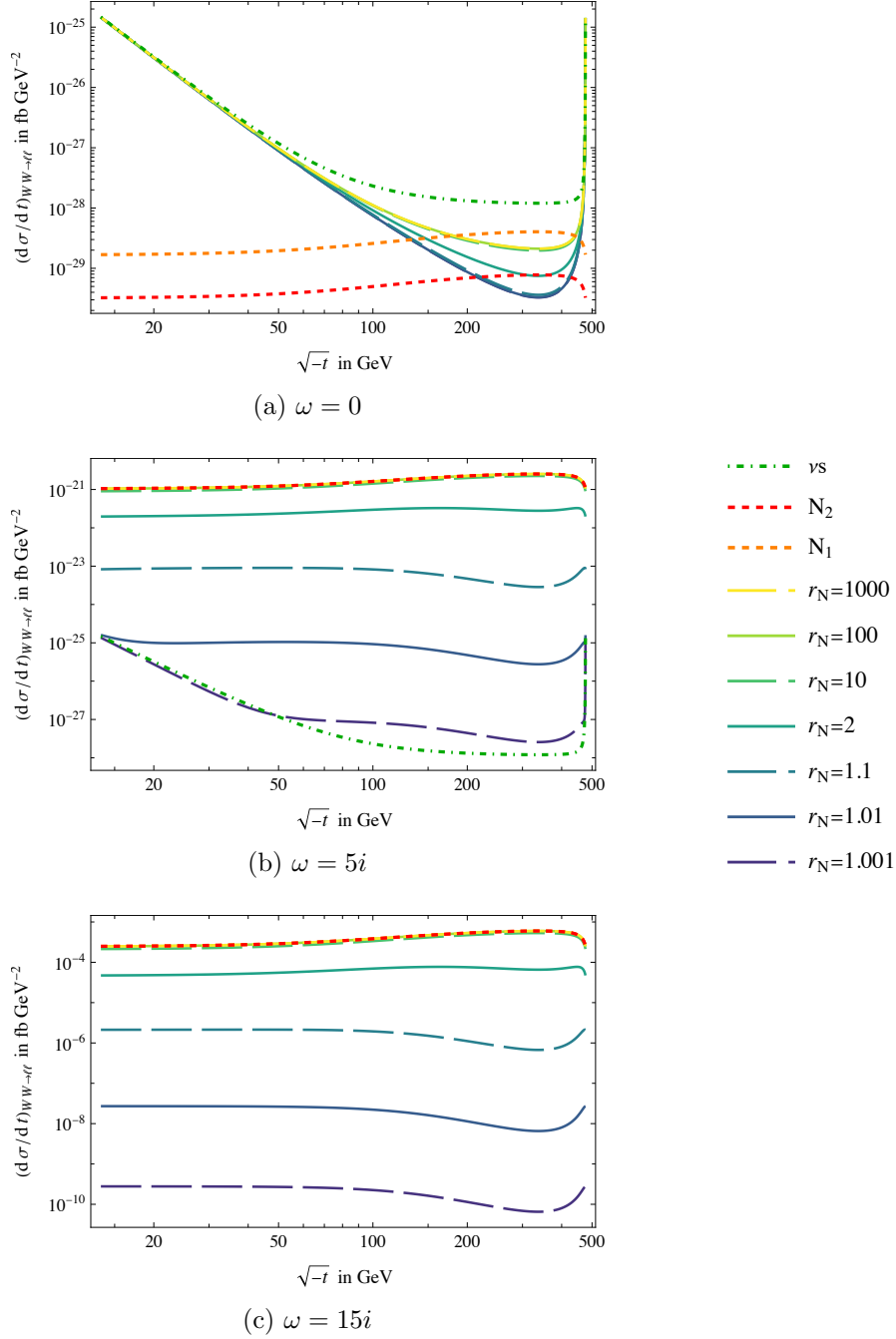


Figure 14: Differential cross section of $W^\pm W^\pm \rightarrow \ell^\pm \ell^\pm$ scattering using the Casas-Ibarra parametrisation of the HNL mixing angles with enhancement parameter $\text{Im}(\omega)$. Here, $r_N = \frac{m_{N2}}{m_{N1}}$ is the mass ratio. The lighter of the two HNL masses $m_{N1} = 150$ GeV and the centre of mass energy is 490 GeV.

This shows that for large Θ , qDL becomes a very good approximation of a fully realistic model. By virtue of this equivalence, for our purposes, the numerical stability of the prior far outweighs the usefulness of considering the full model. This is

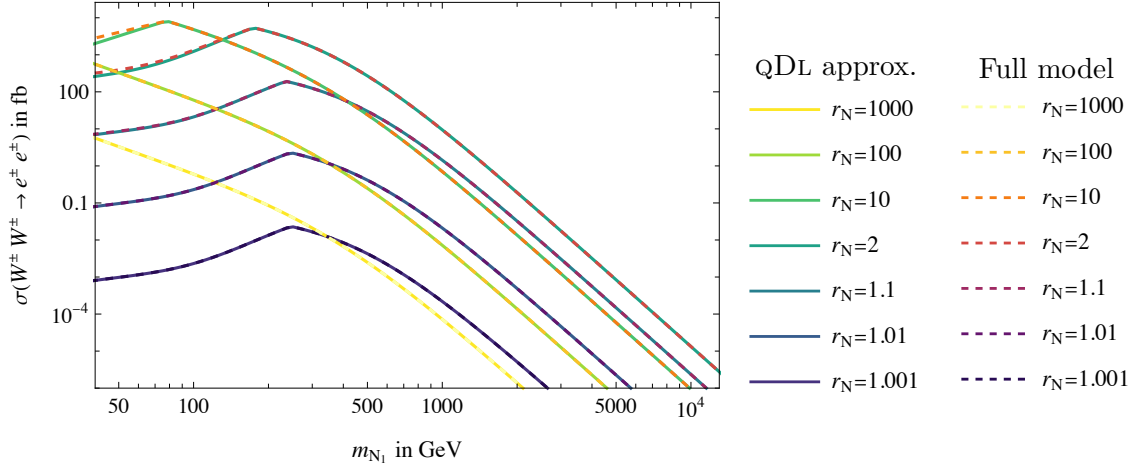


Figure 15: Comparison of $W^\pm W^\pm \rightarrow \ell^\pm \ell^\pm$ cross sections between qDL and fully realistic two HNL neutrino sector model. The data is shown at a maximally admissible mixing angle $\Theta_{\ell 1}$ according to eq. (4.1).

especially true since only large mixing angles have a chance of being detected at the LHC and FCC (see section 4).

D Effective W approximation

In the deduction of the effective W approximation’s parton distribution functions (PDFs) according to [98] (see figure 16 for PDFs at relevant centre of mass energies), one formally assumes decoherence between the polarisation states of individual W “partons”. This means that if contributions due to different polarisation states are on a similar scale — and thus the decoherence assumption is no longer valid — the results at pp level are potentially underestimated by a factor of few².¹⁷

To investigate the validity of the approximation we will thus compare the doubly longitudinally polarised (LL) WW cross section to the doubly transversally polarised (TT) case. As the folding with PDFs involves an integration over different energy regimes, this is important at all relevant centre of mass energies determined by the PDFs in figure 16. Figure 17 shows this for a centre of mass energy on the lower end of the PDF spectrum ($s_{\text{WW}} = 16m_W^2$, figures 17a and 17b) and on the upper end ($s_{\text{WW}} = s_{\text{LHC}}/100$, figures 17c and 17d). We note that for low end energies, the LL cross section becomes dominant for $m_{N_1} \gtrsim 100\text{--}200$ GeV, while at larger energies this is the case for $m_{N_1} \gtrsim 10\text{--}100$ GeV. As pp level validity is determined by validity at all relevant subenergies, only a region of general LL dominance fully meets the assumptions of the effective W approximation. We thus expect accurate results in a

¹⁷This is due to the error occurring in both p involved in the $pp \rightarrow \ell^\pm \ell^\pm jj$ process.

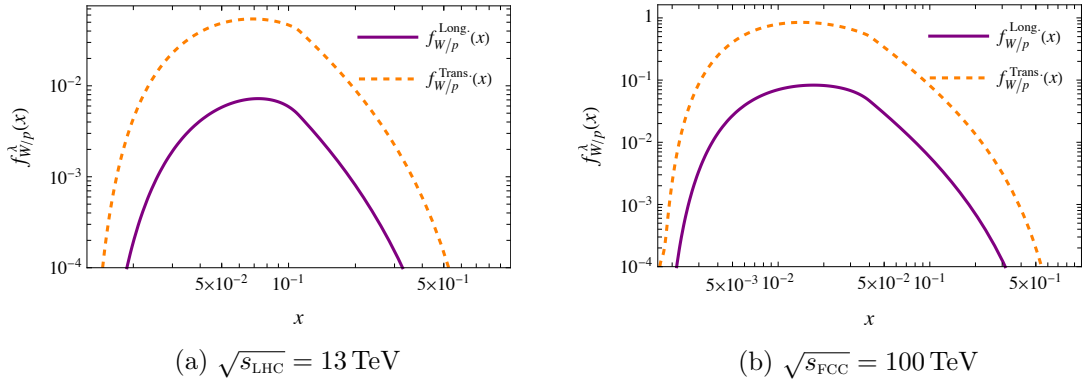


Figure 16: Parton distribution functions of the effective W approximation as prescribed in [98] at LHC (a) and expected FCC centre of mass energy (b). The underlying quark parton distribution functions used were taken from [142].

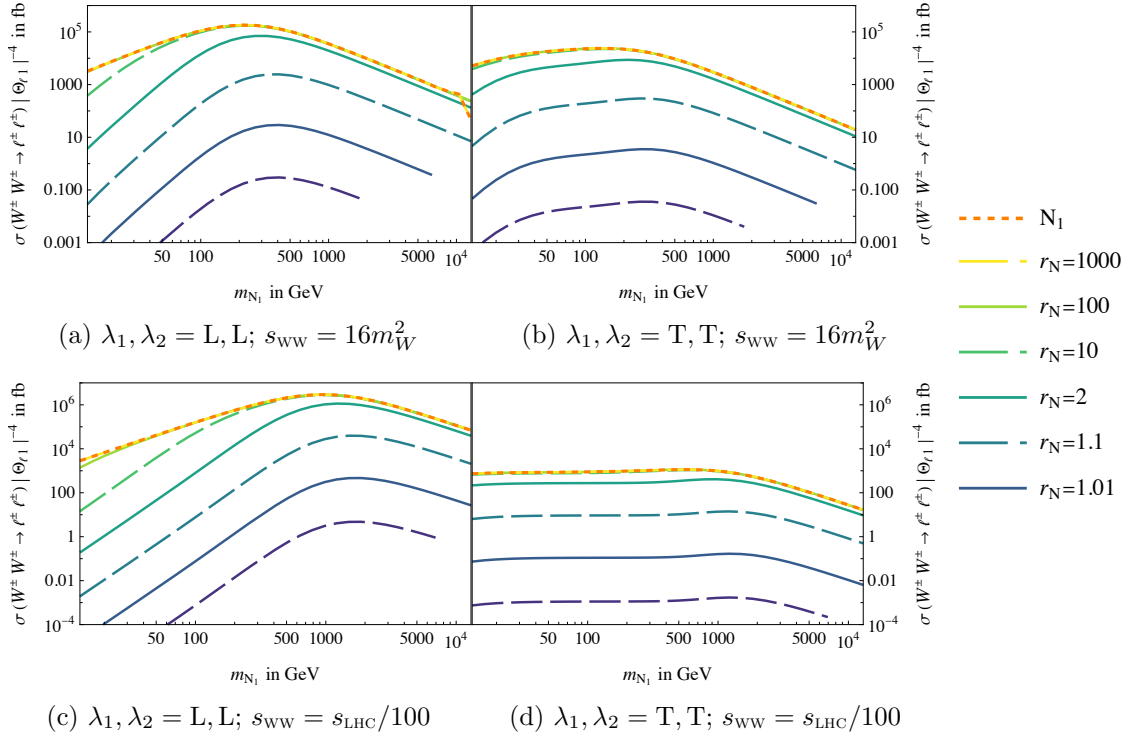


Figure 17: Polarised cross sections of $W^\pm W^\pm \rightarrow \ell^\pm \ell^\pm$. The polarisatinos λ_1, λ_2 are both longitudinal (L, L, left panels) or transversal (T, T, right panels), while the centre of mass energy is $4m_W = 225 \text{ GeV}$ (top panels) or $\sqrt{s_{\text{LHC}}}/10 = 1.3 \text{ TeV}$ (bottom panels). We assume a QDL model with mass ratio r_N .

parameter space of $m_{N_1} \gtrsim 400 \text{ GeV}$, while we expect to underestimate the pp level cross section for smaller m_{N_1} .

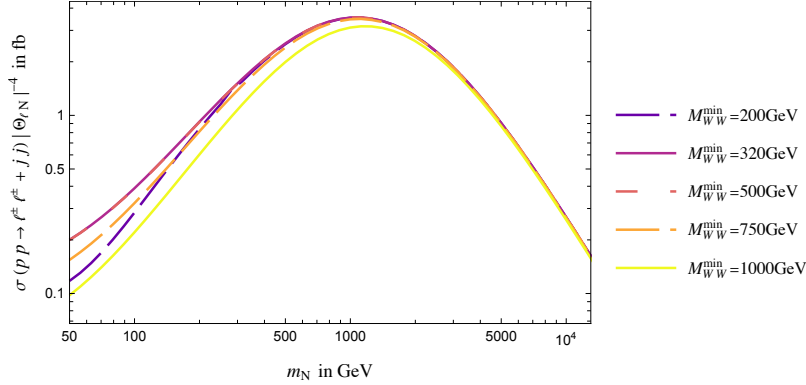


Figure 18: Single isolated HNL pp level WBF cross section at $\sqrt{s_{\text{LHC}}} = 13$ TeV as a function of HNL mass m_N . This is shown for different lower bounds on the integration parameters of the effective W approximation determined by M_{WW} according to eq. (D.1).

It has been, furthermore, pointed out in past literature that in order to achieve numerical stability, the lower limit of the integration [101] has to be set above a certain threshold, rather than to account for minimal production energy. We investigate this by varying the lower limit on

$$x_1 x_2 = \frac{M_{WW}^2}{s_{pp}}. \quad (\text{D.1})$$

This is shown in figure 18, where we have plotted the cross section of a single isolated HNL for different values of M_{WW}^2 at $\sqrt{s_{\text{LHC}}} = 13$ TeV. For small HNL masses $m_N \lesssim 100$ GeV, there is a noticeable dependence on the lower cut-off. We note that the cross section for $M_{WW}^{\text{min}} = 320$ – 500 GeV is largest in this regime, even though we removed part of the integration interval for positive definite functions with respect to e.g. $M_{WW}^{\text{min}} = 200$ GeV. The lines of $M_{WW}^{\text{min}} = 320$ GeV and $M_{WW}^{\text{min}} = 500$ GeV coincide for all mass values m_N . For $m_N \gtrsim$ several 100 GeV, the numerical values are identical for all $M_{WW}^{\text{min}} < 750$ GeV, while the curve of $M_{WW}^{\text{min}} = 750$ GeV lies slightly below the others. The curve representing $M_{WW}^{\text{min}} = 1$ TeV lies below the others by a factor of $\mathcal{O}(10\%)$ for lower m_N converging with the rest at $m_N \simeq$ few TeV.

Overall the effect of the cut-off is only significant in the regime of $m_N \lesssim 100$ GeV. As the focus of this work lies on the regime of $m_N \simeq$ several 100–few 1000 GeV, the influence is thus marginal. Nevertheless, we set the lower limit $M_{WW}^{\text{min}} = 4m_W \simeq 320$ GeV as a benchmark for this work, which corresponds to twice the minimal production energy and is already in a numerically stable regime according to figure 18.

For the case of a single HNL in a phenomenological type-I seesaw, figure 19 compares the resulting cross section deduced using the EWA without any detector-motivated cuts with that given in the NLO in QCD WBF study by Fuks et al. [73]. As expected from the above discussion, the results differ significantly (by a factor of ~ 10) for

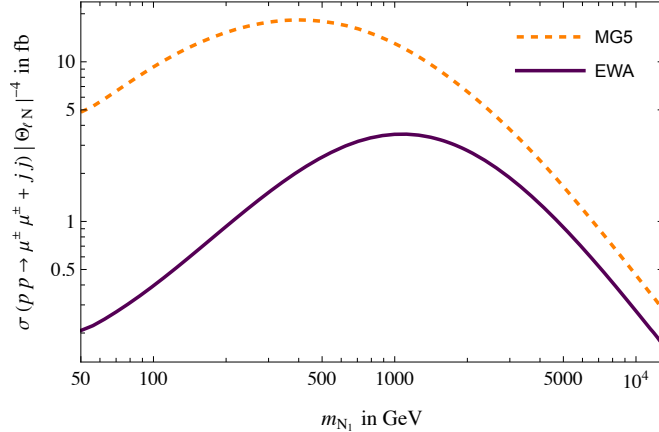


Figure 19: WBF at pp level cross section for a single isolated HNL ($W^\pm W^\pm$ combined). Comparison of MG5_AMC Montecarlo detector simulation by Fuks et al. [73] (dashed orange) and effective W approximation (purple), shown at LHC centre of mass energy $\sqrt{s_{\text{LHC}}} = 13$ TeV.

$m_{N_1} \sim \text{few } 100 \text{ GeV}$. For masses in the TeV-range, however, the results become comparable within order few reaching order several 10 % for $m_{N_1} \sim \text{several TeV}$. As this coincides with the significant mass range of our study, the pp level results presented here can be understood as estimates within $\mathcal{O}(1)$. We highlight that this only affects the absolute scale of our pp level results, while relative differences between different mass ratios r_N stem from analytic treatment at WW level, and will thus hold at pp level as well.

E Potential avenues for future same sign di-lepton searches at colliders

Even though WBF does not look like a promising channel for HNL discovery at the LHC at tree level, it remains to be seen if loop-order corrections to the $W^\pm W^\pm \rightarrow \ell^\pm \ell^\pm$ system could potentially boost the signal. Especially penguin corrections to the $WN\ell$ vertices (similar to [110]) and corrections to the Majorana propagator (similar to those responsible for running of light neutrino masses) could be of interest here.

Another important aspect to investigate is the question of how a tendency toward front-to-back scattering in the WW system for smaller mass ratios translates into angular distributions of the full pp scattering. This will need to be investigated in a full on $2 \rightarrow 4$ simulation of the process as this phenomenon only occurs for $m_{N_1} < \text{few } 100 \text{ GeV}$, which is outside the full validity of the EWA, while all angular dependence is strongly suppressed for HNLs with $m_{N_1} \gtrsim \text{few TeV}$. If indeed front-to-back scattering translates into large lepton pseudorapidities at pp level, the drop

off for smaller r_N with respect to realistic detection prospects could be even more severe than anticipated. However, due to the detection limits at the (HL-)LHC, this question is more relevant for FCC energy level searches.

Another avenue of exploration could be to consider three or more HNLs with similar masses and mixing angles to see if significant LNV effects could be realised in a realistic neutrino sector model. As this greatly opens up the available parameter space, *the single HNL case would not hold as an upper limit.*